Sandra Isabel Nunes Cordeiro

Licenciada em Biologia Celular e Molecular

Antioxidant – loaded mucoadhesive nanoparticles for eye drug delivery: new strategy to reduce the oxidative stress

Dissertação para obtenção do Grau de Mestre em
Genética Molecular e Biomedicina

Orientador(a): Joana Marto, Professora Doutora,
Faculdade de Farmácia, Universidade de Lisboa
Co-orientador(a): Lídia Gonçalves, Professora Doutora,
Faculdade de Farmácia, Universidade de Lisboa

Júri:
Presidente: Prof. Doutor(a) Alexandra Fernandes
Arguente(s): Prof. Doutor(a) Pedro Viana Baptista
Vogal(ais): Prof. Doutor(a) Joana Marto

FACULDADE DE CIÊNCIAS E TECNOLOGIA
UNIVERSIDADE NOVA DE LISBOA

Setembro, 2019

Sandra Isabel Nunes Cordeiro

Licenciada em Biologia Celular e Molecular

Antioxidant – loaded mucoadhesive nanoparticles for eye drug delivery: new strategy to reduce the oxidative stress

Dissertação para obtenção do Grau de Mestre em
Genética Molecular e Biomedicina

Orientador(a): Joana Marto, Professora Doutora,
Faculdade de Farmácia, Universidade de Lisboa
Co-orientador(a): Lídia Gonçalves, Professora Doutora,
Faculdade de Farmácia, Universidade de Lisboa

FACULDADE DE CIÊNCIAS E TECNOLOGIA
UNIVERSIDADE NOVA DE LISBOA

Setembro, 2019

Antioxidant – loaded mucoadhesive nanoparticles for eye drug delivery: new strategy to reduce the oxidative stress

Abstract

There are several techniques of drug delivery to treat ocular diseases, which can be invasive or non-invasive. In the area of the non-invasive techniques, new pharmaceutical strategies based on nanotechnology and mucoadhesive polymers are emerging approaches to reach an efficient treatment of ocular diseases. The aim of this work is to develop novel nanoparticle systems with mucoadhesive properties, intended to encapsulate antioxidant molecules and, aiming to reduce the generation of oxidative stress and consequently ocular diseases. To improve the retention time of antioxidant molecules on the surface of the eye, our strategy involves the use of nanoparticles composed by chitosan and hyaluronic acid, with known mucoadhesive properties.

The optimization strategies involved the development of nanoparticles composition aiming a nanoparticle size lower than 400nm and a positive zeta potential with a high yield. The nanoparticles were characterized by hydrodynamic mean particle size, dispersity index, zeta potential and yield (<350nm, <0.300, >+35mV, >90%, respectively) and the antioxidant encapsulation efficiency and the ophthalmic formulations were characterized in terms of pH, osmolality, viscosity and zeta potential. FTIR and TEM were used to understand better the interactions the nanoparticles components and their morphology, respectively. Mucoadhesion studies achieved by the interaction between the nanoparticles and mucin were conducted using different methods, namely: zeta potential measurements, viscosity measurements and tackiness testing, and they showed a high interaction between them, which means that the nanoparticles are able to increase the residence time in the eye surface. The *in vitro* release drug profiles, through synthetic membranes and pig eyes in Franz diffusion cells of the antioxidants were conducted to understand the kinetic mechanism involved on the drug release profile. The safety and efficacy of the novel formulation were tested *in vitro* using ARPE-19 cell line, presenting a high efficacy of the antioxidant activity and low cytotoxicity.

In conclusion, CS/HA nanoparticles is a promising platform for antioxidants delivery in the eye by increasing its residence time and controlled drug delivery. In the future, *in vitro* experiments would be useful to elucidate the biodistribution of drugs after ophthalmic application and would be also useful the scale-up of the manufacturing processes using a Quality by Design approach.

Keywords: eye drug delivery, nanoparticles, antioxidant, mucoadhesive, chitosan, hyaluronic acid

Resumo

Existem várias técnicas de distribuição de fármacos para o tratamento de doenças oculares e podem ser consideradas como invasivas ou não invasivas. No ramo das técnicas não invasivas estão a surgir novas estratégias farmacêuticas baseadas na nanotecnologia e polímeros mucoadesivos, para o tratamento eficiente de doenças oculares. O objetivo deste trabalho será então o desenvolvimento de novos sistemas de nanoparticulas com propriedades mucoadesivas, destinado a encapsular moléculas antioxidantes e atingir o derradeiro objetivo de reduzir a formação de stress oxidativo e consequentemente de doenças oculares. De forma a aumentar o tempo de retenção das moléculas antioxidantes na superfície do olho, a nossa estratégia passa pelo uso de nanoparticulas compostas por quitosano e ácido hialurónico, que possuem propriedades mucoadesivas.

A optimização do processo de produção das nanoparticulas teve como objectivo a obtenção de um tamanho menor que 400nm e um potencial zeta positivo com elevado rendimento. As nanoparticulas foram caracterizadas através do seu tamanho hidrodinâmico médio, índice de dispersão e rendimento (<350nm, <0.300, >+35mV, >90%, respetivamente) e a eficácia de encapsulação e formulações oftálmicas foram caracterizadas em termos do seu pH, osmolaridade, viscosidade e potencial zeta. Como forma de compreender melhor as interações entre os componentes das nanoparticulas e a sua morfologia foram realizadas as técnicas de FTIR e TEM, respetivamente. Os estudos mucoadesivos conseguidos pela interação entre as nanoparticulas e a mucina resultaram da utilização de diferentes métodos: medição do potencial zeta, medição da viscosidade e teste de aderência. Estes estudos demonstraram uma elevada interação entre as nanoparticulas e a mucina, o que indica que as nanoparticulas são capazes de aumentar o tempo de retenção na superfície do olho. Os perfis de libertação do antioxidante *in vitro* foram realizados através de membranas sintéticas e olhos de porco nas células de difusão de Franz para uma melhor compreensão dos mecanismos de cinética envolvidos nestes perfis. A eficácia e segurança das novas formulações foram testadas *in vitro* utilizando a linhagem celular ARPE-19 para a qual apresentaram uma atividade antioxidante bastante eficaz e baixa citotoxicidade.

Em suma, as nanoparticulas de quitosano e ácido hialurónico são uma plataforma promissora para a distribuição de antioxidantes no olho, uma vez que aumentam o seu tempo de residência no mesmo e controlam a sua distribuição. No futuro, poderão ser úteis experiências *in vitro* para um melhor entendimento da biodistribuição dos fármacos após a sua aplicação oftálmica e ainda a realização de um aumento da escala do processo de produção recorrendo à abordagem de “Quality by Design”.

Palavras-chave: Distribuição de fármacos no olho, nanoparticulas, antioxidantes, mucoadesivo, quitosano, ácido hialurónico

Agradecimentos

A realização desta dissertação para a finalização dos estudos relativos à obtenção do grau de mestre apresentou desafios intelectuais, profissionais e pessoais a ser superados. A superação destes desafios só foi possível com a entreajuda de todos aqueles que contribuíram para que esta dissertação se pudesse realizar. Assim sendo, cabe-me agora expressar o meu profundo agradecimento a todos os que me ajudaram neste percurso e o tornaram mais simples.

À Professora Doutora Joana Marques Marto, minha orientadora principal, por toda a sua ajuda durante a realização da dissertação, pelos seus conselhos, pela sua constante preocupação, por todas as suas dicas que me ajudaram tanto e sobretudo pela amizade que foi desenvolvida. A Professora mostrou-se sempre muito disponível para me guiar e ajudar a ultrapassar dificuldades e foi extraordinária, permitindo-me assim crescer tanto a nível pessoal como profissional. Agradeço também toda a sua receptividade para me esclarecer toda e qualquer dúvida, embora nunca facilitando demasiado o processo de obtenção de respostas, permitindo-me chegar a decisões e conclusões por mim mesma, o que me fez crescer muito enquanto investigadora. Foi um grande privilégio poder ter disfrutado durante este ano da sua companhia e espero que a amizade construída se mantenha para além deste trabalho.

À Professora Doutora Lídia Maria Diogo Gonçalves, minha co-orientadora desta tese, gostaria de demonstrar o meu profundo agradecimento por me ter acompanhado neste percurso e me ter ajudado a superar as mais diversas dificuldades com as quais me fui deparando. Tenho que agradecer por me ter transmitido os seus ensinamentos através do seu trabalho de excelência e ter demonstrado sempre a maior disponibilidade, a maior dedicação e motivação que foram tão importantes para mim durante este tempo. Ajudou-me também a crescer em todos os aspetos e estou-lhe muito grata pela forma como me recebeu. Permitiu-me chegar a decisões e conclusões de forma quase autónoma, dando-me por isso oportunidade de errar e aprender com os meus erros. Foi também um grande privilégio poder ter passado este ano da sua companhia e espero igualmente que a amizade construída se mantenha daqui em diante.

À Beatriz Silva pela sua contribuição na realização do intenso trabalho de laboratório.

À Professora Paula Gonçalves como coordenadora do Mestrado e pela disponibilidade ao longo desta jornada.

A todos os membros do edifício D da Faculdade de Farmácia pela hospitalidade, pela simpatia e pelo convívio durante a realização do trabalho de laboratório, em especial às alunas de Mestrado Ana Sofia Saraiva e Inês Anjos e também à Ana Neves.

Aos meus amigos, em especial à Iolanda Neves, Sofia Carapinha, Catarina Monteiro, Laura Custódio, Ana Bandeiras, Ana Pires e Inês Sousa, por toda a sua paciência, incentivo e ajuda.

À minha mãe e irmão pelo apoio incondicional e orgulho que demonstram por mim todos os dias.

List of Content

List of Figures

List of Tables

Abbreviations

Actino	Actinoquinol
Alamar Blue	7-hydroxy-3H-phenoxazin-3-one 10-oxide
AMD	Age-related Macular Degeneration
BRB	Blood-retinal Barrier
CAT	Catalase
CMC	Carboxy-methyl Cellulose
CS	Chitosan
DHA	Dehydroascorbate
DL	Drug Loading
EE	Encapsulation Efficiency
FR	Free Radical
FTIR	Fourier-transform Infrared Spectroscopy
GI	Gastrointestinal
GPx	Glutathione Peroxidase
GSH	Glutathione
GSSG	Glutathione Disulfide
HA	Hyaluronic Acid
HPMC	Hydroxyl-propyl-methyl Cellulose
MC	Methyl Cellulose
MP	Macular Pigment
MPOD	Macular Pigment Optical Density
MRI	Magnetic Resonance Imaging
MTT	3-(4,5-dimethyl-2-thiazolyl)-2,5-diphenyl-2H-tetrazolium bromide
NIPAAm	N-isopropylacrylamide
NMDA	N-ethyl-D-aspartate
NMR	Nuclear Magnetic Resonance
NP	Nanoparticle
OS	Oxidative Stress
PBS	Phosphate-buffered Saline
PdI	Polydispersity Index
PEO	Poly (ethylene oxide)
PI	Propidium Iodide
PLGA	Poly-lactic-co-glycolic Acid
PPO	Poly (propylene oxide)
QUR	Quercetin
RES	Resveratrol
RGCs	Retinal Ganglion Cells
ROS	Reactive Oxygen Species
RP	Retinitis Pigmentosa

RPE	Retinal Pigment Epithelium
SD	Standard Deviation
SDS	Sodium Dodecyl Sulfate
SOD	Superoxide Dismutase
TEM	Transmission Electron Microscopy
TNF	Tumour Necrosis Factor
Vit. A	Vitamin A
Vit. C	Vitamin C
Vit. E	Vitamin E
ZP	Zeta Potential

1. Literature Overview

1.1. The Eye Anatomy

The human eye has an approximately globular, quite complex, structure and its tissues have a distinct structure. [1,2] The ocular tissues are very compact and have a couple of cell layers of thickness. The eye is also composed by barriers with the function to keep the systemic circulation separate from ocular tissues. [1]

The eye is divided in 2 segments, the anterior, which is responsible for collecting and focusing light, and the posterior segment, which has the function of detecting light. The anterior segment of the eye includes the lens, lachrymal system, iris, aqueous humour, ciliary body, pupil, conjunctiva and the cornea. On the other hand, the posterior segment includes the retina, choroid, sclera, macula, fovea, optic nerve and the gelatinous vitreous humour. [1]

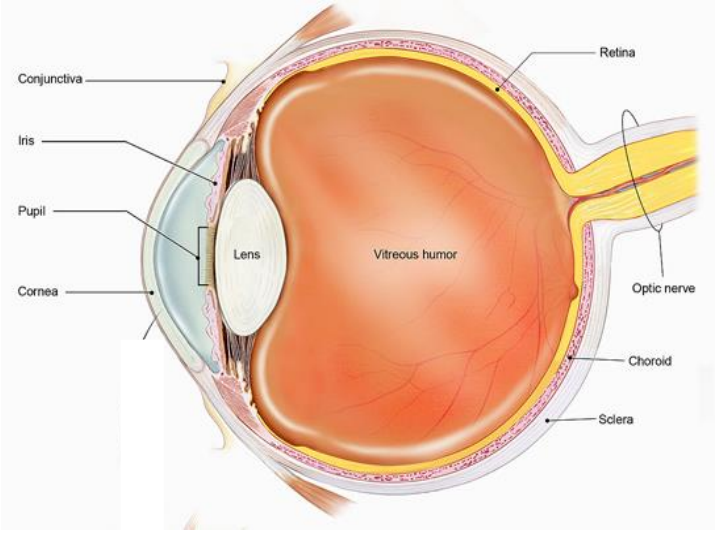

Figure 1.1: Structure of the human eye. Adapted from [3]

The eye is constituted by three concentric adjoining tissue layers: an outermost layer, which provides mechanical strength to the eye; an anterior portion, cornea, that is transparent to visible light and has the function of focusing the light on the retina; an posterior portion, sclera; and a middle layer, termed uvea, a pigmented layer that comprises the iris and ciliary body in the anterior portion and the vascular choroid in the posterior portion. [1]

The cornea is the primary barrier for topical drug absorption, allowing only small molecules to penetrate and a clear transparent epithelial collagenous structure with refractive power of the light rays to focus them on the retina. [1,2] The cornea comprises 5 layers: the corneal epithelium (provides an optimal surface for the tear film to spread across the surface of the eye to keep it moist and healthy), Bowman’s membrane (transparent film of tissue), stroma (composed by water and collagen, which gives strength, elasticity and forms to the cornea), Descemet's membrane (with protective barrier function against infection and injuries) and the corneal endothelium (maintains the fluid content within the cornea). [1,2,3,4]

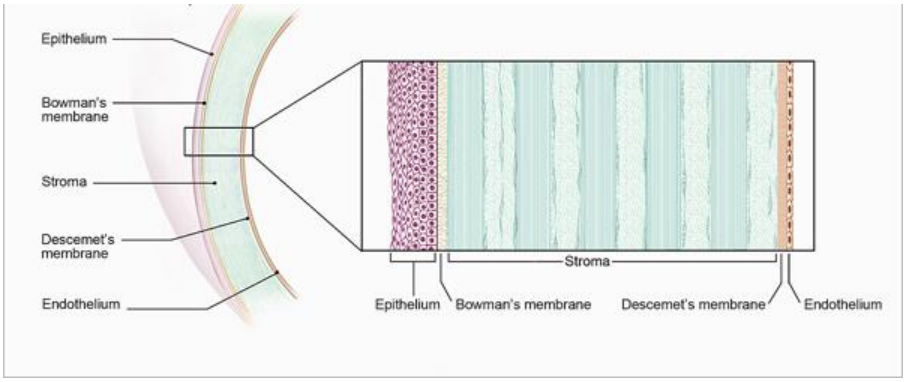

Figure 1.2: Constitution of the cornea from a human eye. Adapted from [3]

All the layers have specific characteristics in their constitution that limit diffusion across the cornea, in addition to that, in the outer surface of the cornea exists a constant flow of a tear film, which all together result in a low bioavailability of 1–7% for most approved drugs. [1]

The iris is the visible coloured part of the eye and it is supplied by parasympathetic and sympathetic nerves. It has the function of controlling the amount of light entering the eye by contracting the pupil, when there is parasympathetic stimulation, and dilating the pupil, when it has sympathetic stimulation. The choroid is a vast network of capillaries, with the functions of supplying the retina with nutrients and absorbing unused radiation. [1,2]

The retina is composed by layers with photoreceptors and retinal ganglion cells (RGCs), which are normally composed by a cell body, dendrites and an axon, and it detects and transduces light signal to the brain by forming an image through the light that has passed until it. Retina is a barrier to macromolecules. [1,2,5]

The optic nerve has the function of helping in vision by transmitting information from the cells of the retina. [2] The sclera is a membrane that maintains the shape of the eye and gives the attachment to the extrinsic muscle of the eye, what makes it also a barrier to diffusion of macromolecules. [1,2]

1.2. Structure of the tear film

The tear film, constant flow that exists on the cornea, has three major functionalities, which are to provide good optics and vision, protect the front of the eye from the environment and allow the lids to slide comfortably. [6] The tear film is constituted by three main layers, the oily or lipid layer, the aqueous layer and the mucous layer (Figure 1.3). [6]

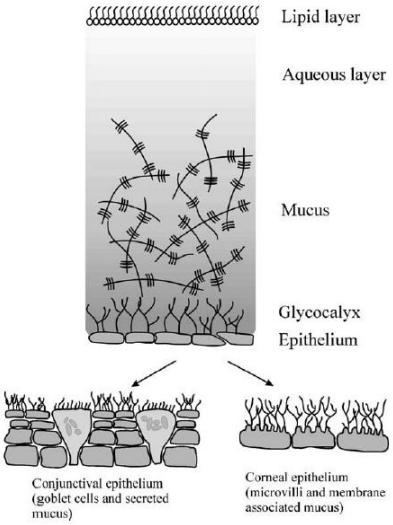

Figure 1.3: Main layers and other important elements of tear film of the human eye. Adapted from [7]

The tear film also has microvilli (Figure 1.3) of different types and dimensions depending on the maturity of the cells that enhance the cohesion and stability of the tear film. The normal tear present pH values around 5.2 to 9.3, being its mean value of 7.4. [7]

1.2.1. The Lipid Layer

The lipid layer, the outer layer, has the role of preventing tears from breaking up and evaporating and help them spread over the cornea. The Meibomian glands (tubule-acinar and holocrine glands) secrete an oil (clear and run freely), with a combination of polar and nonpolar lipids, like the Meibomian lipid, that constitute the lipid layer. [6,8,9] Consequently their secretion is delivered to the marginal reservoirs, allowing that the secretion from the Meibomian glands to spread into the aqueous layer, when the eye blinks. [7,8]

1.2.2. The Aqueous Layer

The aqueous layer is considered to be the middle layer and has the essential elements for wound repair and resistance against infection. The lachrymal glands and smaller glands of the conjunctiva are responsible for the formation of the layer. [6] This layer is not only constituted by an aqueous media but also by various water soluble and water insoluble components (electrolytes, proteins, peptides and small molecule metabolites). [10]

1.2.3. The Mucous Layer

The mucous layer has in its principal constituent mucins that are important for reducing the surface tension of the tears and give the non-Newtonian rheological behavior of the tear film. [7,8] This layer can also be considered a diffusion barrier due to its degree of network entanglement but, at the same time, the negative charges of the mucin at physiological pH due to its sialic acid end chains allow their combination to the cationic substances. The structure of

the mucus is formed essentially by glycoproteins (like mucin), proteins, lipids, electrolytes, enzymes, mucopolysacchrides and water. [7]

Several types of mucins have been reported to be part of the structure of the human eye. These types can be classified essentially in three groups, the membrane-spanning, membrane-associated and secreted. This last group of mucins may be separated according to their capacity to form associations with polymers. They can be soluble mucins or gel-forming mucins (MUC2, 5AC, 5B and 6), which exhibit rheological properties. The membrane-associated mucins are MUC1, 3A, 3B, 4, 12 and 13 and have three domains in their structure, a cytoplasmic domain, a hydrophobic domain and an extracellular domain. [7] The most important mucins are the MUC5AC, secreted by the conjunctival goblet cells and the MUC1, MUC4 and MUC16, which generate the glycocalyx of the ocular surface epithelia. [8,11]

1.3. Oxidative stress

In our daily routines we are exposed to oxidative stress (OS) through environment by products of metabolism and lifestyle factors, being our tissues more exposed and vulnerable to OS, like the anterior segment of the eye, cornea, lens, and trabecular meshwork. [12,13] Free radicals (FRs), like reactive oxygen species (ROS), are common products that result from normal aerobic cellular metabolism (mitochondrial electron transport chain) or from the incidence of UV radiation. The human body has antioxidant defense systems that get overwhelmed with aging, resulting in increased OS and damage to tissues of the eye and onset of various ocular pathologies, for example glaucoma. [12,13,14,15] The OS stimulates an imbalance between the production of ROS and the antioxidant power of the cell, which leads to cellular damage by inducing DNA damage and consequently the apoptosis in a variety of cell types. [12,13] OS has a significant contribution in the development of neurodegeneration through ROS attack to neural cells, which may cause several disorders such as Alzheimer's disease, Parkinson's disease, aging, macular degeneration, glaucoma and many others. [15]

The eyes are mostly affected by the incidence of UV radiation, which is responsible for some pathogenesis of the ocular tissues. Therefore, the eye has excellent antioxidant defenses that act at different levels. Ocular tissues that are less exposed to light have a poor antioxidant defense and ocular tissues that are constantly exposed to light have a strong antioxidant defense. [13]

1.3.1. Neurodegenerative diseases

Neurodegeneration can be caused by an imbalanced defense mechanism of antioxidants, overproduction or incorporation of FRs from environment to living systems and is manifested in a sensorial or functional loss in the neural cells. [15]

One of the most known neurodegenerative diseases in the eye are the retinal neurodegenerative diseases, which are divided in those that affect the outer retina and the ones that affect the inner retina. The ones that affect the outer retina are characterized by the death of the primary sensory neurons (photoreceptor neurons), which are responsible for detecting light.

On the other hand, the neurodegenerative diseases in the inner retina affect both bipolar cells and RGCs, which are responsible for connecting the retina to visual pathways in the brain. [16]

Several outer retinal diseases can appear in the population, like age-related macular degeneration (AMD), which causes photoreceptor loss through retinal pigment epithelium (RPE) dysfunction, and retinitis pigmentosa (RP), that affect both photoreceptors and RPE. [16] AMD has some similarities to the Alzheimer's disease, such as Aβ in drusen and protein misfolding that can lead to OS, uncontrolled inflammation and imbalanced angiogenesis. [5]

The most known inner retinal degenerative disease is the glaucoma that consists in the primarily RGCs death (preceded by axonal atrophy and deficits in axonal transport), what will cause the degeneration of the optic nerve and the loss of the retinal connection to the brain. [5,16]

1.3.1.1. Therapeutics for Neurodegenerative diseases

One of the new perspectives of therapeutics for neurodegenerative diseases is the use of antioxidants, because they have the capacity to eradicate the FRs by neutralization. [15] The pathways of antioxidants delivery and metabolism into the different tissues of the eye have not been completely understood yet. [12]

Another therapeutic perspective is the use of some therapies in AMD that are already used in brain diseases, because of the similarities shown between these two types of diseases, such as, some approaches that reduce Aβ load and improve cognitive performance. [5] It may be also considered the therapy of targeting glial cells since changing its response to OS could reduce axonal damage and RGC soma death. [14]

1.3.1.1.1. Antioxidant agents

The antioxidant defense systems use two principal types of antioxidants to fight against the OS the enzymatic and non-enzymatic antioxidants. Enzymatic antioxidants catalyze electron transference from a substrate toward ROS. The main antioxidant enzymes known are superoxide dismutase (SOD), catalase (CAT) and glutathione peroxidase (GPx), each one of them catalyzes the reduction of a particular type of ROS. SOD catalyzes the dismutation of $O_2^{\bullet -}$ into H_2O_2 and O_2. This enzyme has three isoforms of metalloproteins: the isoforms Cu-SOD and Zn-SOD, which are located in the cytosol and extracellular fluid, and the isoform Mn-SOD, which is located in the mitochondrial matrix. [17,18]

CAT is a hemoprotein that contains four heme groups. It can be found in peroxisomes mitochondria and cytoplasm and catalyzes the conversion of H_2O_2 into H_2O and O_2. CAT has higher affinity than GPx to H_2O_2 when this is found in high concentrations. [17]

GPx can reduce H_2O_2 into water and organic hydroperoxides into alcohol, using reduced glutathione (GSH) as electron donor. This enzyme has four known isoforms: cellular GPx, extracellular or plasmatic GPx, phospholipid hydroperoxide GPx, and gastrointestinal GPx. [17,18]

The other type of antioxidants, the nonenzymatic antioxidants, act by donating an electron to a FR in order to stabilize it and create chemical species that are less noxious to cell integrity.

The principal nonenzymatic antioxidants described until now are ascorbic acid, vitamin E (Vit. E), vitamin A (Vit. A), GSH and crocin. Ascorbic acid reduce $O_2^{\bullet -}$, $OH^{\bullet -}$ and lipid hydroperoxide into more stable forms and help to recycle α-tocopheryl radical to α-tocopherol. In this process dehydroascorbate anion radical is produced from the transformation of the ascorbate anion and it is later reduced by dehydroascorbate reductase and GSH returning it to native state. Ascorbate also has pro-oxidant properties in the presence of excessive concentrations of ions Fe^{3+} and Cu^{2+}. [17] It is also essential for collagen synthesis and has anti-inflammatory properties. [12]

Vit. E is a generic name for a family of eight compounds, four tocopherols, and four tocotrienols. The α-tocopherol is the most active antioxidant. The α-tocopherol converts $O_2^{\bullet -}$, $OH^{\bullet -}$ and $LOO^{\bullet}$ into less reactive molecules. In order to stabilize ROS, the α-tocopherol is converted into the α-tocopheryl radical, whose shape is stable. This radical can be regenerated to its original form through reactions mediated by vitamin C (Vit. C), GSH, and lipoic acid, which keep α-tocopherol in its reduced state in instances of OS. [17]

Vit. A has a major precursor, the β-carotene, which is the most efficient neutralizer of O_2. Vit. A main function is to convert $O_2^{\bullet -}$ and $LOO^{\bullet}$ into less reactive substances. [17]

GSH principal aim is to transfer electrons to oxidized specie such as hydroxyl radicals and carbonyls, becoming in turn an oxidized product (GSSG). GSH can act as co-substrate of GPx in the removal of H_2O_2 and organic peroxides. [17] GSH protects de protein thiol groups and mediates the recycling of dehydroascorbate (DHA) to ascorbic acid in this active form. [12,13] The DHA is toxic to the lens and can cause the formation of senile and diabetic cataract. [12]

Table 1.1: Analysis of the levels and influence of antioxidants in several ocular disease. Adapted from [17]

Antioxidants	Objective	Conclusion	References
Enzymes: GPx and SOD.	Determine plasma levels of antioxidant enzymes related with cataract and AMD (2584 subjects, >60 years).	High levels of plasma GPx leads to AMD and cataract prevalence and high levels of plasma SOD to cataract prevalence.	**[19]**
Carotenoids, α-tocopherol, and γ-tocopherol.	Assess the relation of serum carotenoids and tocopherols levels to the incidence of cataract (400 subjects of 50 to 86 years, 7 years follow-up.).	High serum levels of tocopherols are associated with low risk of cataract.	**[20]**
Vit. C, Vit. E, α and β-carotene, y-copene, lutein, zeaxanthin, and β-cryptoxanthin.	To determine plasma levels of some vitamins and carotenoids related with cataract risk incidence (372 subjects of 66 to 75 years).	High levels of α-carotene, β-carotene, lycopene and lutein were associated with low risk of cataract.	**[21]**

Antioxidants	Objective	Conclusion	References
Vit. C, Vit. E, riboflavin, β-carotene, lutein, and zeaxanthin.	To assess the relation between usual nutrient intake, plasma vitamins concentration and subsequently diagnosed age-related nuclear lens opacities (478 women of 53 to 73 years).	High Vit. C intake is associated with low risk of cataract incidence. High Vit. C and Vit. E plasma concentrations are associated with low lenticular opacity.	**[22]**
Lutein, zeaxanthin, Vit. C, and α-tocopherol.	To investigate whether serum levels of antioxidants influence the lens optical density (376 subjects of 18 to 75 years)	High serum levels of lutein and zeaxanthin may retard aging of the lens.	**[23]**
Enzymes: SOD and GPx.	To determine the association between antioxidant enzymes activity and incidence of cataract (1947 subjects, >60 years).	High levels of plasma GPx and SOD were associated with high cataract incidence.	**[24]**
Macular carotenoids, meso-zeaxanthin and coantioxidants.	To evaluate the impact of supplemental macular carotenoids combined with co-antioxidants on the visual function of patients with non-advanced AMD (121 participants).	Antioxidant supplementation results in significant increases in macular pigment (MP) and improvements in contrast sensitiity and other measures of visual function.	**[25]**
Macular carotenoids, lutein, zeaxanthin and meso-zeaxanthin.	To evaluate the antioxidant and anti-inflammatory capabilities of the macular carotenoids, lutein, zeaxanthin and meso-zeaxanthin (59 young healthy subjects, 12 months follow up).	Supplementation with the macular carotenoids significantly reduces stress, cortisol, and symptoms of suboptimal emotional and physical health.	**[26]**
Macular carotenoids, lutein,	To investigate whether increasing macular pigment optical density (MPOD) could enhance lateral	Increases in MPOD led to enhanced lateral inhibitory processes. Improvement in contrast sensitivity with	**[27]**

Antioxidants	Objective	Conclusion	References
zeaxanthin and mesozeaxanthin.	inhibitory processes, and thereby improve contrast sensitivity (59 subjects of 18 to 25 years).	increases in MPOD appears to involve enhancement of the fundamental physiological systems that give rise to edge detection.	
Zeaxanthin	To analyze MP amount and distribution in those patients receiving oral zeaxanthin supplementation in a randomized, open-label, interventional trial (8 subjects of 38 to 79 years with macular telangiectasia Type 2).	Zeaxanthin supplementation does not result in any visual benefit on the patients and does not reestablish a normal peaked distribution of MP in the fovea. One patient developed a novel, reversible, crystalline maculopathy in response to zeaxanthin supplementation.	**[28]**

There are several anti-oxidant drugs used in therapeutics like edaravone, ebselen, flavonoids, SOD, GSH, N-acetylcyteine, ascorbic acid and α-tocopherol. The treatment with edaravone is applied to cerebral infarctions and it is administrated intravenously. The edaravone functions are to scavenge ROS and protect the cellular membrane from oxidative damage. Edaravone has been tested in clinical trials for the treatment of amyotrophic lateral sclerosis. Ebselen has a peroxidase-like activity and it is used in the treatment against brain function deterioration. Flavonoids have anti-oxidative effects and it is thought that they may have a role in the prevention of cancer and cardiovascular disease, but human body poorly absorbs them so they have little or no direct antioxidant value in humans. SOD has been used in its modified forms to make it a longer serum half-life. GSH is used to treat chronic liver diseases and cataract and has intravenous administration. N-acetylcysteine originates cysteine by hydrolysis, thus the increase of intracellular GSH levels. N-acetylcysteine is also used to treat over-doses of acetaminophen and improve the bronchial mucous fluidity. Ascorbic acid and tocopherol are used as vitamins but not as anti-oxidants, in clinical terms. [29]

Resveratrol (RES) and quercetin (QUR) may also be used as therapeutic agents due to their properties. RES, it is capable to do FR neutralization, vascular enhancing and activation of serotonins and inhibition of endothelia, and, in the case of QUR, it is a flavonoid and it is able to prevent cataract formation, inhibiting the formation of choroidal neovascularization, treating the AMD and promoting anti-angiogenic activity. According to S. Natesan et. al, when these two agents are used simultaneously in a mucoadhesive polymeric drug delivery system of chitosan

(CS) and polyethylene glycol modified CS nanoparticles, it is observed an increase of the bioavailability of RES and it was possible to reduce the intra ocular pressure for the treatment of glaucoma. [30]

1.3.1.1.1.1. Crocin

Saffron, the dry stigmas of the plant *Crocus sativus L.*, has been used in traditional medicines for the treatment of numerous illnesses, like tumors. Because of its powerful antioxidant activity, saffron extract could also be useful in the treatment of brain neurodegenerative disorders. [31]

The major components of saffron are safranal, crocin and picrocrocin, which are responsible for its aroma, colour and bitter taste, respectively. [32] The extract contains many carotenoids such as crocetin, di-(β-D-glucosyl)-ester (dicrocin), crocetin-(β-D-gentiobiosyl)-(β-D-glucosyl)-ester (tricrocin) and crocetin-di-(β-D-gentiobiosyl)-ester (crocin). [33] These carotenoids scavenge FRs, especially superoxide anions and thereby may protect cells from OS, as was seen in colorectal cancer and hepatocellular carcinoma both *in vitro* and *in vivo*. [31,32]

Crocin ($C_{44}H_{64}O_{24}$) is a rare carotenoid found in nature, which can easily be dissolved in water and, due to that, it has wider application as a colorant in food and medicine, in comparison to other carotenoids. [34] It is an ethanol-extractable component of *Crocus sativus L.* shown to selectively antagonize the inhibitory effect of ethanol on N-ethyl-D-aspartate (NMDA) receptor–mediated responses in hippocampus neurons and to have anti-proliferation and pro-apoptotic effects against HepG2 and gastric adenocarcinoma cells. [32,35] Crocin can also suppress tumour necrosis factor (TNF)-α-induced apoptosis of PC12 cells by modulating mRNA expressions of Bcl-2 family proteins. [33]

1.3.1.1.1.2. Actinoquinol

Actinoquinol, actino, ($C_{11}H_{11}NO_4S$) is a chemical compound and an UV absorber. When actino is combined with hyaluronic acid, HA, (an anionic non-sulfated mucopolysaccharide) in eye drops, it can provide protection to the eye against damaging effect of UVB radiation. [36,37] The actino-HA eye drops decrease changes in corneal optics and suppress oxidative damage in the UVB-irradiated cornea. [37]

1.4. Drug Delivery for Ophthalmic Applications

There are several techniques of drug delivery used to treating posterior ocular disease, such as intravitreal injection, subretinal injection, subconjunctival injection and topical administration. However, all of these methods have various risks. Thus, a better approach still needs to be developed. Non-invasive drug delivery methods, like topical delivery, could potentially eliminate the risks of injection into the eyes but their development has been challenging due to the unique anatomy and physiology of the eye, which limits the bioavailability of these non-invasive treatments. [38,39]

One of the major challenges in ophthalmic drug delivery development is to overcome the physical barriers and blood–ocular barriers of the eye because they are inherent and unique, in the way that they protect the eye from the invasions of environmental toxicants and microorganisms. [39]

Recent studies provide a way to overcome the limitations of drug delivery systems mentioned before through the development of nanostructures capable of encapsulation and delivering drugs to the eye. [39]

1.4.1. Nanoparticles

Nanoparticles (NPs) are nanostructures capable of encapsulating and can penetrate through different biological barriers of the eye for delivering drugs. NPs have small sizes ranging from 1 to 1000nm and can be produced through chemical processes or a simple self-assembly process (involving techniques such as nanoprecipitation, emulsion, dialysis, polymerization method, dispersion of polymers, coacervation or ionic gelation method, in aqueous medium) to control the release of therapeutic agents. [39,40,41] In the ophthalmological applications, the size of these nanocarriers with drug loading is important to avoid a foreign body sensation after administration. [39,40] The main advantages of using drug-loaded NPs in the treatment of ocular diseases are to enhance bioavailability of topical administration, achieve controlled release, targeted delivery and ultimately improve therapeutic efficacy, conducing to lower dosage requirements, less dosing frequency with benefits for the patients. [39,42]

Some of the properties of the NPs are important factors in ocular delivery, such as the surface charge of the NPs, which determine their distribution in different regions of the eye, the size of the NPs, they need to be small enough to penetrate the ocular barriers, and the long-term release effect of NPs, which reduce the frequency of drug administration. [39,40]

Several types of nanocarriers have been studied especially degradable NPs made with polymers, such as CS NP, poly-lactic-co-glycolic acid (PLGA) NP, cellulose derivatives (Methyl cellulose (MC), hydroxyl-propyl-methyl cellulose (HPMC), and carboxy-methyl cellulose (CMC)), xyloglucan, N-isopropylacrylamide-based derivatives, poloxamers, alginates and gelatine NPs. [39,40,42,43]

CS is a polysaccharide copolymer comprised of glucosamine and N-acetylglucosamine and has excellent tolerance and penetration of the corneal surface due to its mucoadhesive property and ability to open tight junctions. They can be administrated by topical administration and corneal stroma and subretinal injections. [39]

PLGA NPs are constituted by a copolymer of poly lactic acid and poly glycolic acid and they are a highly biocompatible, biodegradable and controllable material. These NPs confer protection of encapsulated drugs from rapid inactivation, maintenance of slow drug release due to polymer degradation and targeting of specific regions or cells by surface modification. They can be administrated by topical administration and intravitreal injections. [39]

Cellulose is a water-insoluble polysaccharide, composed by β (1,4)-linked D-glucose units. Some of the most known are the MC, HPMC and CMC. These derivatives are always combined with *in situ* gelling polymers to been used in ocular delivery. [43]

N-isopropylacrylamide (NIPAAm) is a homopolymer and one of its derivatives is the poly-N-isopropylacrylamide. This derivative has been combined with CS to form a thermosensitive gel system. [43]

Poloxamers are non-ionic polymers composed by a hydrophobic chain of poly (propylene oxide) and two hydrophilic chains of poly (ethylene oxide) (PEO-PPO-PEO). These polymers can form thermos-reversible gels. [43]

Alginates are constituted by a (1,4) linked β-D-mannuronic acid (M) and α-L-guluronic acid (G) residues, which makes it a co-polysaccharide. Alginate has a better efficacy when combined with poloxamers and HPMC. [43]

NPs are usually sent to three principal pathways, after its instillation: tear turnover, cornea/anterior region and nasolacrimal drainage (Figure 1.4). [39]

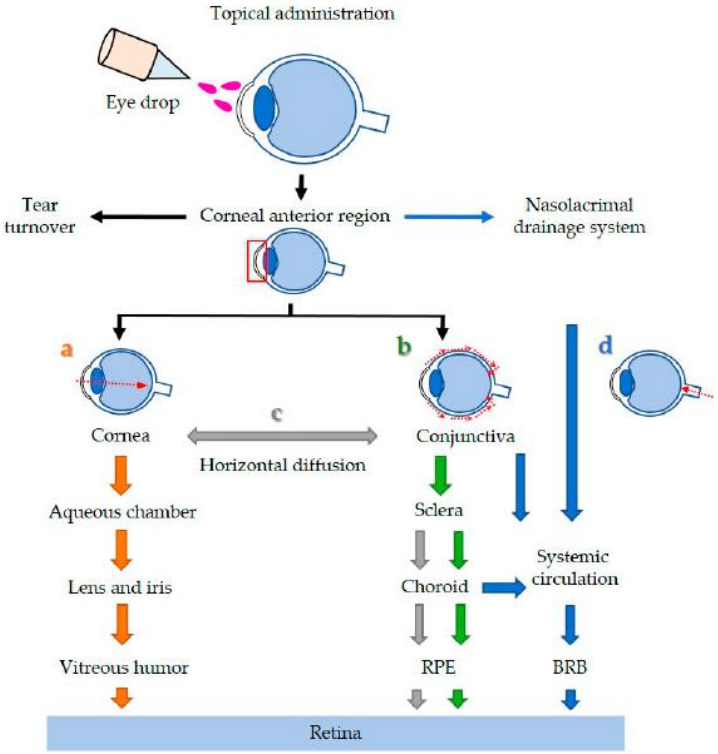

Figure 1.4: Possible routes of drug delivery to the retina via topical administration. RPE: retinal pigment epithelium; BRB: blood–retinal barrier. Adapted from [39]

1.5. Mucoadhesion and mucoadhesive properties

A mucoadhesive property of the polymers is one of the important factors for the ocular drug delivery with nanoparticulated systems since have enhanced bioavailability and increase the velocity of absorption. The term bioadhesion implies the attachment of a drug carrier system to a specified biological location that may be a mucus coat, which in that case is called mucoadhesion. [44] Mucoadhesion is characterized by the interaction between the adhesive molecules (like a synthetic or natural polymer) and mucus glycoprotein (mucin), for example the ocular delivery

systems and mucins present in the eye, followed by the formation of secondary chemical bonds, in the case of the eye non-covalent bonds. [44,45,46]

The mucoadhesive polymers used can be water-soluble or water-insoluble, this last type has hydrophilic groups (such as hydroxyl, carboxyl, amide and sulfate) that interact with water molecules and expand the polymer network to a more flexible and mobile state. When the mucoadhesive polymer in contact with the hydrophilic mucus is stretched and entangled by various interactions (like hydrogen bonding and hydrophobic or electrostatic interactions), it matches its active adhesive sites to those on the substrate. [44,46] The characteristics that a polymer should have in order to obtain adhesion to the mucous layer are the following ones: sufficient quantities of hydrogen-bounding chemical groups, anionic surface charges, high molecular weight, high chain flexibility and induction of spreading by surface tensions. [44,47] Mucoadhesive polymers need to be non-irritant and it and its degradation products should be nontoxic. [47]

The mucoadhesion mechanism has two steps: the contact stage and the consolidation stage. The contact stage is characterised by the spreading and swelling of the formulation when the initial contact between the two layers occurs. The consolidation step focuses in the activation of the mucoadhesive material by moisture and its bonding. [47]

It has been formulated liquid eye drops with *in situ* hydrogels, that the process of gelification occurs when in contact with the eye, giving a response to environmental changes and increasing bioavailability and the contact time between drug and mucosa. [46,48] The mucoadhesion has some important characteristics that give advantage over other delivery systems, such as prolongation of resident time, drug targeting and intimate contact between dosage form and the absorptive mucosa. [47]

1.5.1. Polymers

Polymers with mucoadhesive properties used to develop drug delivery systems are a way to increase the drug bioavailability, through the increase of its retention time. [46,49] In addition to that characteristic of mucoadhesive polymers they also demonstrated protective and healing properties to epithelial cells. [8] In the case of drug delivery in the eye, these polymers have the function of attaching themselves to corneal or conjunctival mucin, through non-covalent bonds, until the mucin turnover occurs and eliminates the polymer. Because of that, the mucin-mucin bond has to be weaker than the mucin-polymer bond. If the mucin-polymer is too strong, the polymer offers resistance to blinking and eye movements and it will feel uncomfortable in the eye. [46]

As previously referred, the mucoadhesive polymers can be water-soluble or water-insoluble. The water-soluble ones are slowly dissolved in the tear film while the water-insoluble ones remain attach to mucin until its replacement. [46] Nowadays, the CS and the HA are two of the mucoadhesive polymers most used in drug delivery. [7]

1.5.1.1. Chitosan

Chitosan (CS) is derived from chitin deacetylation and present mucoadhesive properties and as well as pH response, with pseudoplastic and viscoelastic behavior. [7,45,49] The mucoadhesive properties presented by CS are based on electrostatic interactions (hydrogen bounds) between its positively charged amino groups and the negatively charged sialic acid residues of mucin, which prolong the residence time of the polymer in the cornea of the eye. [45,49,50] CS is also biocompatible, biodegradable and shows antimicrobial and wound healing properties. [45]

The CS may be administrated in liquid dosage forms in viscous solutions or in particulate systems, like microspheres and nanospheres. For viscous solutions, it was synthesized various CS derivatives, like N-trimethyl CS and N-carboxymethyl CS, in order to improve the mucoadhesive properties observed in CS. The studies show that the N-trimethyl derivative was the most effective, the CS chloride precipitates in the tear film and the N-carboxymethyl CS did not enhance the penetration. On the order hand, the particulate systems increase delivery to external ocular tissues without compromising inner ocular structures and systemic drug exposure and they allow the contact of the NPs with corneal/conjunctival epithelium and they may enter in it by paracellular or transcellular pathways. The delivery of the CS molecules in this kind of systems is mediated by the biodegradation of the polymer that depends on the degree of acetylation of the CS molecules. [50]

1.5.1.2. Hyaluronic Acid

Hyaluronic Acid (HA) is a high molecular linear polymer composed of long chains of repeating disaccharide units of N-acetylglucosamine and glucuronic acid and it is present in the synovial fluid and extracellular matrix of connective tissues in vertebrates. [45,51,52,53] HA is used in drug delivery for optimized systems and improves its biocompatibility, like the case of the microcapsules and the CS microspheres used for the delivery of plasmid DNA and monoclonal antibodies in gene transfer and site specific targeting. [53]

HA is frequently used in ocular drug delivery systems, like eye drops, because of its characteristics like biocompatibility, biodegradability and mucoadhesive properties that allow to extend the pre-corneal residence time. [45,54] However, the eye drops have several limitations, like the need of frequent application. [51] HA also confers to the corneal epithelium protection against dehydration, reduction of healing time, reduction of the inflammatory response caused by dehydration and lubrication of the ocular surface. [54]

The HA is capable to interact selectively with cell-surface HA receptors such as CD44, which are present in the ocular epithelium and promote wound healing. [45] This characteristic of HA enables cell internalization of different systems, which make HA a very useful compound for transfection approaches. [52]

1.5.2. Important Factors to Mucoadhesion

There are several factors that may affect the mucoadhesion, such as the nature of the polymer and of the surrounding media. [44,47] One of them is the hydrophilicity of the mucoadhesive polymers, which helps in the exposure of the potential anchor sites and to a more efficient penetration of the substrate. [44] The molecular weight of the polymers can be a problem since it is necessary a polymer with high molecular weight (100 000kDaltons or more) to obtain high mucoadhesion. [44,47] The optimum concentration of polymer used corresponds to the best mucoadhesion and that concentration changes with the physical properties of the polymer. [44] A critical factor for interpenetration and entanglement is the number of polymer chains, higher the number, higher the mucoadhesive strength. [47]

Another factor that influences the mucoadhesion is the pH value, as mucoadhesive systems are constituted by ionizable groups and carboxylic acid functionalities, this last one in the case of polyanions. [44] Mucoadhesion is also influenced by the forces that are applied when the initial contact occurs and by the exact moment of its initial contact. Higher forces mean a higher mucoadhesivity and a higher time of contact leads to a higher swelling and interpenetration of the polymer chains. The swelling depends on the concentration of the polymer, the presence of water (large quantities of water may lead to a formation of a slippery layer that cause the decreasing of mucoadhesivity) and the concentration of ionic species. [44,47]

1.5.3. Techniques used for the Assessment of Mucoadhesion

There are various methods that allow the study of mucoadhesion. The tensile test, shear strength and peel strength are the methods that are used to measure the force of attachment. [47] The tensile test consists in the application of a force perpendicularly to the tissue/adhesive interface creating a tensile stress on it. This technique gives us the force of separation necessary to remove the tissue/adhesive material. The shear strength is based in the same principle of force application as the tensile test, but with the objective of create a shear stress that will reorient the force in order to act along the joint interface. These two methods measure the mechanical properties of the system. The third method, peel strength, is used when the mucoadhesive system is formulated as a patch and measure the resistance of the peeling force, through the determination of the energy required to detach the patch from the substrate. [44]

Another method for evaluation of mucoadhesion is the rheological technique. Although it should not be used as a stand-alone method, this technique allows determining the rheological interaction between a polymer gel and mucin solution through the analyses of the flow and deformation of materials, which is better when the gel and the solution are mixed. [44]

There are some tests that can be executed *in vivo*. The most common are the gastrointestinal (GI) transit times of bioadhesive-coated particles and drug release from *in situ* bioadhesive devices. [44] The GI transit study normally implies the use of radio-opaque markers encapsulated in bioadhesive, so that the total GI residence time is monitored without affecting normal GI motility. [47] This technique uses X-ray, gamma scintigraphy, magnetic resonance imaging (MRI) and other noninvasive methods to execute the monitoring. [44]

1.5.4. Mucoadhesion Theories of Polymer Attachment

It is really difficult to define one theory to explain the polymer attachment by mucoadhesion, and so there are different theories that can justify some of the experimental observations made in mucoadhesive studies, although these theories can't explain all the interaction that constitute the bioadhesive bond. Therefore, five theories stand out from the others: the wetting theory, the diffusion theory, the electronic theory, the absorption theory and the mechanical interlocking theory. [44] The first two theories are encompassed in the physical methods, while the electronic and absorption theories belong to the chemical methods. [47]

1.5.4.1. Wetting Theory

The wetting theory is normally applied to liquids or low viscosity mucoadhesive systems, once this theory explains it as an embedding process, in which the adhesive agents penetrate in the surface irregularities of the substrate and produce adhesive anchors through intermolecular interactions and interfacial tension. [44,55] These adhesive agents must overcome the surface tension effects of the substrate in order to have a fluid movement on it. [44] Therefore, the lower the contact angle, the greater the affinity of the liquid to the substrate surface is because the liquid drop spreads across the surface due to cohesive forces. [55,47] The Young equation allows to determinate the contact angle:

$$\gamma_{SG} = \gamma_{SL} + \gamma_{LG} \cos\theta \quad (1)$$

Where γ_{SG} is the interfacial tension between solid and medium, γ_{SL} is the interfacial tension between solid and liquid, γ_{LG} is the interfacial tension and θ is the contact angle between solid and liquid interface. [55]

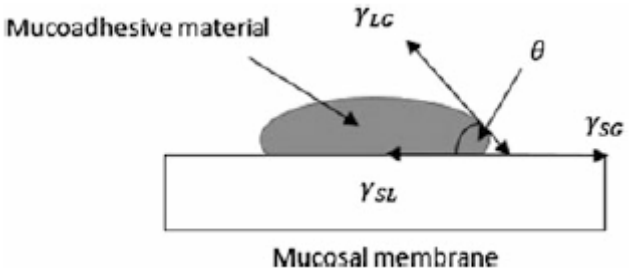

Figure 1.5: Schematic representation of the forces that act in a wetting theory system. Adapted from [55]

1.5.4.2. Electronic Theory

The electrostatic theory defends that there is a transfer of electrons between the adhesive surface and the adhering surface, which leads to the occurrence of an electrical double layer at the interface and attractive forces that are able to maintain the contact between the two layers. [44]

1.5.4.3. Diffusion Theory

This theory explains the formation of a semi-permanent bond between the polymeric chains of the mucoadhesive material and the glycoprotein mucin chains by penetration and entanglement of both layers. [44,55] The penetration of both layers have an equilibrium penetration depth that is achieved when the mucoadhesive matrix is formed, through the existence of concentration gradients and different diffusion coefficients. First occur the approaching of the polymer chain to the mucus layer, secondly happens the interpenetration of the polymer into the mucus layer and finally the polymer chains and the mucus layer contact by physical-chemical forces. [44]

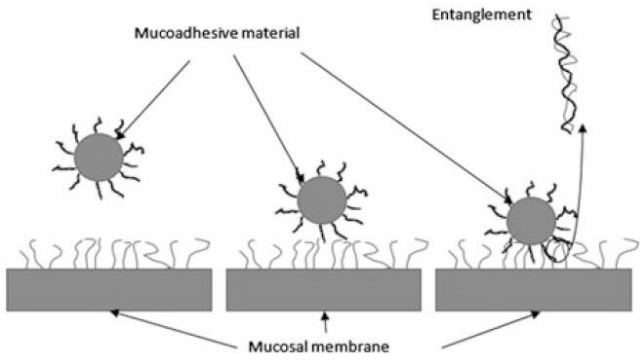

Figure 1.6: Schematic of the steps of diffusion theory. Adapted from [55]

1.5.4.4. Absorption Theory

The absorption theory says that, after the initial contact between the surfaces of both materials, the forces present on their surface, such as van der Waal's forces, hydrogen bonding, and hydrophobic bonding, act between the chemical structures of both of them, resulting in adherence of the two materials. When these forces operate in simultaneous, the adherence of the materials is stronger. [44]

1.5.4.5. Mechanical Interlocking Theory

This theory defends that there is a formation of an interlocked structure, which leads to adhesion, what is caused by the diffusion of the liquid that will adhere to the micro-cracks and irregularities of the substrate. [47] This theory is only applied to adhesion between liquid and rough surface or surface rich in pores. [55]

1.6. Evaluation of the Product Efficacy

1.6.1.*In vitro* models

The cell culture systems and animal models allow a better understanding of the cell biology, tissue morphology, mechanisms of diseases, drug action, protein production and the development of tissue engineering because they provide a simple, fast and cost-effective tool to avoid large scale. [56,57] These studies normally use primary cells that can come from the donor's material or culture deposited in cell banks, when isolated from living organisms, which may contain populations of different cell types (being important to select just the right cell type for the

study). The cell lines from cell bank are normally immortalized cells once they are established from various types of cancer cell lines. [56]

There are two types of cell culture models used for different studies, the two-dimensional (2D) monolayer cell culture model and the three-dimensional (3D) cell culture model, being the 2D model the standard method. [56] The 3D model presents an advantage in comparison to the 2D model because it is able to replicate the *in vivo* environment that surrounds the cells through an extracellular matrix, being able to predict *in vivo* responses. [57]

The adherent 2D cell cultures present themselves as a monolayer of cells in a culture flask, attached to the surface of the flask. They usually are monocultures, allowing the study of only one type of cells that are not able to be differentiate, and have unlimited access to the ingredients of the medium such as oxygen, nutrients, metabolites and signal molecules. [56]

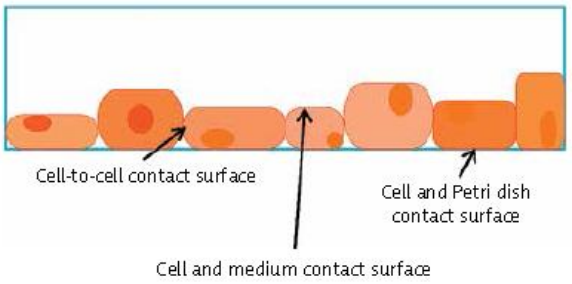

Figure 1.7: Representation of the interaction that an adherent cell is able to execute. Adapted from [56]

The cells of the outermost layer of the retina, the RPE cells, are responsible for the transport of nutrients from vascular choroid, the formation of the blood-retinal barrier and absorption of scattered light. The ARPE-19 is a human RPE cell line (primary culture) that has rapid rate of proliferation distinguishes it from the other primary RPE cultures. [58]

2. Materials and Methods

2.1. Materials

Low-molecular weight CS was obtain from VegeTec (CSU), HA kindly offered by Soliance (Paris, France), Sodium chloride (NaCl) from AppliChem (AppliChem, Germany), actino from TCI (TCI E0339), purified water was of Milli-Rx quality (Merck Millipore, Darmstadt, Germany) and crocin, 10mM phosphate-buffered saline (PBS) and mucin from porcine stomach were obtained from Sigma-Aldrich (Irvine, UK). All other reagents and solvents were of the purest grade available, and were generally used without further treatment.

The ARPE-19 (ATCC® CRL-2302™) cell line was obtained from the American Type Cell Culture collection (Manassas, VA, USA). Cell culture media and supplements were from Gibco (Thermo Fisher Scientific, Paisley, UK). The dyes used in the cytotoxicity studies come from Sigma-Aldrich (Irvine, UK) and from molecular Probes (Thermo Fisher Scientific, Paisley, UK).

2.2. Methods

2.2.1. Manufacturing Process

The CS/HA, CS/HA/crocin, CS/Ha/actino and CS/HA/crocin/actino NPs formulations were prepared using an ionic gelation technique, as previously described by Cadete, A. et al. [59]. Low-molecular weight CS 1% (w/v) was prepared in a 1% (v/v) acetic acid aqueous solution. The CS solution was diluted in NaCl 0.9% to prepare CS solutions of 1mg/mL, the pH value of was adjusted to 5.0 using 1N NaOH. For the production of CS/HA formulations, the solutions of HA with different molecular mass were prepared (HA 50kDaltons, HA 1000kDaltons, HA 3000kDaltons and HA eye at 10mg/mL, final concentration of 1mg/mL). The CS/HA/crocin formulations were obtained through the addiction of the solutions of HA, H_2O and crocin (crocin at 1mg/mL) to the CS solution at different amounts. The same process was used to obtain CS/HA/actino formulations but the actino solution was added to the CS solution instead of being added to the HA eye solution. The CS/HA/crocin/actino formulation was obtained by a mix of the two processes of formation of CS/HA/crocin and CS/HA/actino formulations. All the solutions previously mentioned were prepared at room temperature and using purified water.

The scale up of the CS/HA/crocin, CS/HA/actino and CS/HA/crocin/actino formulations was evaluated, the homogenization process was done by magnetic stirrer, with high shear homogenization (ultra-turrax T10basic at 1400rpm, IKA-Labortechnik, Germany) for 15 minutes and 2 minutes by manual stirring.

2.2.2. Nanoparticles characterization

The particle size and size distribution (polydispersity index, PdI) were determined by dynamic light scattering using a Zetasizer Nanoseries Nano S (Malvern Instruments, Malvern, UK). The Zeta Potential (ZP) was measured using a Zetasizer Nanoseries Nano Z (Malvern Instruments, Malvern, UK). The yield was calculated by the measure of the absorbance at 600nm using FLUOstar Omega (The Microplate Reader Company, BMG LABTECH, Germany). All the

measurements were executed at room temperature and in triplicate (n=3), the results are presented as the mean ± standard deviation (SD).

2.2.2.1. Encapsulation Evaluation

After the formulation of the CS/HA/crocin, CS/HA/actino and CS/HA/crocin/actino NPs, 1mL of the formulation solution was centrifuged at 15000xg during 15 minutes, 200µL of the supernatant of each solution added to a well of a 96-wells plate , in triplicates (n=3). The amount of free drug present in the supernatant was measured using UV-Visible spectrophotometry (FLUOstar Omega, BMGLabtech, Ortenberg, Germany) at 324nm for crocin and 305nm for actino. A calibration curve with different concentrations of crocin and actino was prepared, between 500µg/mL to 244ng/mL, for crocin, and 250µg/mL to 244ng/mL, for actino, for the concentration of free drug calculation. The crocin encapsulation efficiency (EE) and drug loading (DL) of NPs were determinate using the following equations:

$$\%EE = \frac{(C_t - C_f)}{C_t} \times 100 \quad (2)$$

$$\%DL = \frac{(C_t - C_f)}{W_{np}} \times 100 \quad (3)$$

where C_f is the concentration of free crocin, C_t is the total concentration added to the NP formulation and W_{np} is the weight of the NPs.

2.2.2.2. Fourier-transform infrared spectroscopy (FTIR)

For the FTIR analyses, it was necessary to freeze dried the NPs. Formulations were frozen and freeze-dried for 24h (Christ Alpha 1–4, Osterode am Harz, Germany), before freeze-drying, trehalose (10% w/v) was added to all formulations as a cryoprotector.

To prepare samples for FTIR spectra the freeze dried NPs formulations were mixed with KBr, after compression the tablets were analysed. Then the tablets were FTIR analysis in an IRAffinity-1 (Shimadzu Corporation). All spectra were recorded at room temperature at the resolution of $4cm^{-1}$ and 50 times scanning between 4000 and $500cm^{-1}$.

2.2.2.3. Transmission Electron Microscopy (TEM)

The particles morphology analysis was performed using TEM according to the method described by Ferreira et al. [60] The optimized formulations were applied to the cooper grid, dried at room temperature and analysed on Hitachi 8100 with ThermoNoran light elements EDS detector and digital image acquisition at Instituto Superior Técnico from University of Lisbon.

2.2.3. Stability Testing

For the stability test, NP formulations were characterized and analysed in terms of size, PdI and ZP through the Zetasizer Nanoseries Nano S (for the size and PdI) and Zetasizer Nanoseries Nano Z (for ZP) equipments, during 32 days (0, 8, 15 and 32 days). All the

measurements were executed at 4ºC and in triplicate (n=3), the results that were obtained are presented as the mean ± SD.

2.2.4. *In vitro* Assays

2.2.4.1. Cell Culture Condition

The ARPE-19 (human retinal pigment epithelial cell line, ATCC® CRL-2302™) cell line is maintained in RPMI 1640 culture medium (Thermo Fisher Scientific, Paisley, UK) supplemented with 10% fetal bovine serum (Thermo Fisher Scientific, Paisley, UK), 100units/mL of penicillin G (sodium salt) (Life Technologies, Paisley, UK), 100µg/mL of streptomycin sulfate (Thermo Fisher Scientific, Paisley, UK) and 2mM L-glutamine (Thermo Fisher Scientific, Paisley, UK) at 37ºC and 5% CO2.

2.2.4.2. Cytotoxicity

The cytotoxicity tests of the NP formulations were obtained using propidium iodide (PI) exclusion assay, resazurin reduction 7-hydroxy-3H-phenoxazin-3-one 10-oxide (Alamar blue) and 3-(4,5-dimethyl-2-thiazolyl)-2,5-diphenyl-2H-tetrazolium bromide (MTT) reduction assays. [45,61,62] PI is a red fluorescent probe that is a cell membrane impermeant, and, therefore, only penetrates membrane integrity-compromised cells. When PI does gain access to nucleic acids and intercalates them, its fluorescence increases dramatically allowing to identify membrane integrity-compromised cells. Resazurin is a weakly fluorescent blue dye that is reduced by viable cells into the pink-colored and highly red fluorescent resorufin. MTT is a yellow, water-soluble tetrazolium dye and its assay was used to investigate the mitochondrial function through its conversion to a water-insoluble and purple compound, formazan, by viable cells.

For the cytotoxicity studies, there must be a preparation and incubation periods of the cells and formulations. Firstly, the ARPE-19 cells were inoculated in sterile flat-bottom 96-well tissue culture plates (Greiner, Kremsmünster, Austria) in RPMI 1640 culture medium with all the supplements at a cell density of $2x10^5$cells/mL. Then the cells were incubated during 24h at 37ºC and 5% of CO_2. Medium is replaced by fresh medium and the different formulations are added to the respective wells (10µL/well). Each formulation was tested in eight wells (n=8). The cells were incubated again for 24h at the same incubation conditions. The negative control was the culture medium, and positive control was sodium dodecyl sulfate (SDS) at 1mg/mL.

After the time of exposure of the cells to the formulations, the medium was replaced by fresh medium and added 0.3µM of PI (stock solution 1.5mM in DMSO). Fluorescence was measured in microplate reader (FLUOstar Omega, BMGLabtech, Ortenberg, Germany) and then the Alamar Blue assay was performed. The 5mM of Alamar Blue was added to the wells and after 2h of incubation the fluorescence was measured in a fluorescence microplate reader (FLUOstar Omega). Finally, the MTT assay was executed by the addition of 0.25mg/mL of MTT to the wells. The cells were incubated for more 2h and then the medium was removed and 100µL of DMSO was used to solubilise the crystals of reduced formazan and the absorbance was measured at 570nm in microplate reader.

The relative cells viability (%) compared to control cells was calculated by three different ways, one for PI uptake assay (4), other for the Alamar Blue (5) assay and a last one for MTT assay (6).

$$\text{PI uptake} = \frac{\text{Fluorescence}_{\text{sample}}}{\text{Fluorescence}_{\text{control}}} \quad (4)$$

$$\text{Cell viability (\%)} = \frac{\text{Fluorescence}_{\text{sample}}}{\text{Fluorescence}_{\text{control}}} \times 100 \quad (5)$$

$$\text{Cell viability (\%)} = \frac{[(\text{Absorvance})]_{\text{sample}}}{[(\text{Absorvance})]_{\text{control}}} \times 100 \quad (6)$$

2.2.5. *In vitro* release and permeation studies

The *in vitro* release and permeation studies were executed by dialyses membranes and Franz cells methods described below.

2.2.5.1. Dialyses membranes

The dialyses method consists in a tube of dialysis membrane (cut-off of 300Daltons) where 1mL of formulation with crocin and free crocin solution, in triplicates (n=3), were introduced and placed in a close receptor compartment containing 15mL of PBS solution (10mM phosphate buffer saline at pH 7.4) with continuous horizontal shaking at 300rpm and 37ºC. At regular time intervals (from 15 to 15min until the 1h and from hour to hour until the 24h), samples were withdraw and the same volume was immediately replaced with fresh PBS solution maintained at the same temperature. The amount of crocin released was evaluated by UV-spectrophotometry in a microplate reader (FLUOstar Omega) at 324nm.

2.2.5.2. Franz Diffusion Cells

The Franz-type diffusion cells with cellulose membranes and pig eyes (scleras) permit to evaluate the release and permeation of the formulations with crocin and free crocin solution. This method separates the donor and receptor phases, being the first one filled with 200µL of each sample, six samples of each formulation and solution (n=6), and the second one with 3 to 3.5mL of PSB solution at pH 7.4. The Franz cells were incubated at 37ºC with magnetic stirring at 300rpm. From 15 to 15 min until the 1h and from hour to hour until the 24h, it was collected 200µL of the receptor phase and replaced the same amount of volume of PBS solution maintained at the same temperature. The collected samples were used to determinate the amount crocin release through the analysis by UV-spectrophotometry in a microplate reader (FLUOstar Omega) at 324nm. The percentage of cumulative amount of crocin (Q_t) permeated through the membrane (% µg/cm^2) was plotted as a function of time and determined using equation (7):

$$Q_t(\%) = \frac{V_r \times C_t + \sum_{t=0}^{t-1} V_S \times C_i}{A_M} \times \frac{100}{\mu gCF} \quad (7)$$

where C_t is the crocin concentration of the receptor solution at each sampling time, C_i is the concentration at each sampling time, V_r is the volume of the receptor solution and V_s the volume of the sample. The A_M value is the membrane area ($1cm^2$). The weight of CF (µg) corresponds to

$$CF\ (\mu g) = \frac{m_{formulation/solution}\ \text{in Franz cell}\ (g) \times C_{formulation/solution}(mg/g)}{D_{formulation/solution}} \times 1000 \qquad (8)$$

where $m_{formulation/solution}$ is the mass of formulation/solution in the Franz cell, $C_{formulation/solution}$ is the concentration of the formulation/solution and $D_{formulation/solution}$ is the density of the formulation/solution.

As a way to evaluate the mechanism of the crocin released from the NPs, the *in vitro* release data obtained were computed using DDsolver [63], which is an excel-plugin module, and fitted to four different kinetic models.

(9) Zero order kinetics

$Q_t = Q_0 + K_0 t$

where Q_0 is the initial amount of crocin, Q_t is the cumulative amount of drug release at time t and K_0 is the zero order release constant

(10) First order kinetics

$$\log Q_t = \log Q_0 - \frac{K_1 t}{2.303}$$

where Q0 is the initial amount of crocin, Qt is the cumulative amount of drug release at time t and K_1 is the first order release constant

(11) Higuchi model

$Q_t = K_H \sqrt{t}$

where Q_t is the cumulative amount of drug release at time t and K_H is the Higuchi constant

(12) Korsmeyer-Peppas model

$F = K_{KP} \times t_n$

where K_{KP} is the release constant incorporating structural and geometric characteristics of the drug-dosage form and n is the diffusional exponent indicating the drug-release mechanism

The model that best fits the experimental data was selected based on the highest correlation coefficient (R^2) values and lowest Akaike Information Criterion (AIC).

2.2.6. Mucoadhesion studies

These studies were carried out using three different methods: viscometry, rheology and ZP.

2.2.6.1. Ostwald viscometer

For this method were considered the viscosity of the formulations diluted in water in a 1:1 ratio, of the formulations added to mucin in a 1:1 ratio and of mucin dispersion in water (1mg/mL). Each measure was repeated three times (n=3) and measured at 25ºC, using a capillary Ostwald Viscometer. The viscosity component due to bioadhesion or rheological synergism parameter ($\Delta\eta$) was calculated with the equation (13) [64]:

$$\Delta\eta = \eta_{mix} - (\eta_{muc} + \eta_{pol}) \quad (13)$$

where η_{mix} is the viscosity of the formulation-mucin mixture (mPa.s); η_{pol} is the viscosity of the formulation having the same concentration as in the mixture; η_{muc} is the viscosity of mucin dispersion having the same concentration as in the mixture (mPa.s).

2.2.6.2. Rotational Rheometer

The rheological characteristics of the formulations were examined using a controlled stress Malvern Kinexus Rheometer (Malvern Instruments, Malvern, UK). The adhesive strength was also measured with a plate and plate geometry. It was used a toolkit with the conditions of 0.1mm/s, 5mm and 0.15mm of GAP at 20-25ºC. All the measurements were executed six times (n=6), data are presented as the mean ± SD.

2.2.6.3. Zeta Potential

Other method used to evaluate the interaction between the formulations and mucin is the measurement of the ZP of the formulations with and without mucin. All the measurements were executed at room temperature and in triplicate (n=3), data are presented as the mean ± SD.

2.2.7. *In vitro* Assays

2.2.7.1. Oxidative stress tests

The intracellular ROS production was determined using the 2',7'dichlorofluorescein diacetate (H_2DCFDA, ThermoFisher Scientific, Paisley, UK)) probe. The ARPE-19 cells were inoculated in sterile flat-bottom 96-well tissue culture plates (Greiner, Kremsmünster, Austria) in RPMI 1640 culture medium with all the supplements at a cell density of $2x10^5$cells/mL were incubated during 24h at 37ºC and 5% of CO_2. The probe is added at with 20µM of to the wells. After 30 minutes of incubation at the same conditions, the medium is replaced by fresh medium and the different formulations are added to the respective wells.

It was evaluated the reduction of the ROS through two different methods of induction of ROS production: chemical induction (H_2O_2) and physical induction (UV radiation incidence). Hydrogen peroxide solution (AppliChem, Darmstadt, Germany) at 500µM was added to the cells and ascorbic acid at 1mg/mL was used as a positive control and the culture medium as a negative control. The cells were incubate for 1h. The physical induction of the ROS production was carried out through 15 minutes of UV radiation incidence using the same controls. ROS levels were determined using a florescence microplate reader at excitation 485nm and emission 520nm wavelengths (FLUOstar Omega).

The relative ROS production percentage compared to control cells was calculated and expressed as shown in the equation (14).

$$\text{Fluorescence ratio} = \frac{\text{Fluorescence}_{\text{exposed cells}}}{\text{Fluorescence}_{\text{unexposed control}}} \quad (14)$$

2.2.7.2. Nanoparticles uptake

For studying the cellular uptake, 500µL of $2x10^5$cells/mL were seeded in a glass slide into 24-well tissue culture plates and incubated overnight, at 37ºC and 5% CO_2. The NPs were produced using CS* labelled covalently with Oregon Green dye and then placed in the respective wells, eight wells for each NP formulation (n=8). After that, the cells were incubated for 2h at 37ºC and 5% CO_2. After incubation, cells were washed three times with PBS containing 20mM Glycine (Bio Rad, USA) at pH 7.4. Then the cells were fixed with 4% paraformaldehyde for 15min and, washed again with PBS. The cells were permeated with 1% Triton X-100 for 2-5min and washed again. Finally, it was added the 300units of Phalloidin-TRITC for 30min and washed.

Glass cover slips containing cells were mounted with fluorescent mounting medium (ProLong Antifade, Invitrogen, UK) containing DAPI for nucleus labelling. Cells were observed and micro photographed in a Zeiss Axioskop 4.0 fluorescence microscope (Zeiss, Germany). Free imaging software ImageJ was used for microscopy data analysis.

2.2.8. Statistical Data Analysis

Statistical evaluation of data was performed using one-way analysis of variance (ANOVA). The Tukey–Kramer multiple comparison tests (GraphPad PRISM 5 software, La Jolla, CA, USA) was used to compare the significance of the difference between the groups, and a $p<0.05$ was accepted as significant.

3. Results and Discussion

3.1. Manufacturing Process and Nanoparticles characterization

The NP formulations with mucoadhesive polymers have some characteristics that make them a good choice for this kind of delivery system. Among others, these polymers are nontoxic, biodegradable, they are able to encapsulate drug molecules, protect the drug from degradation, prolong the residence time and bioavailability of the encapsulated drug in the ocular surface and constitute a non-invasive drug delivery system. [38,39,45] In this research work were prepared NPs of CS and HA aiming to interact with the ophthalmic mucosal barrier and to facilitate the transport of the antioxidants described in the present work.

The NP formulations were prepared by ionic gelation technique, the complexation between oppositely charged macromolecules, like establishment of hydrogen and ionic bonds between the positively charged amino groups of CS and carboxyl groups of HA. [45,60] Firstly, there were tested different mass proportions of CS and HA, different HA, which differ in their molecular weight (HA 50kDaltons, HA 1000kDaltons, HA 3000kDaltons and HA eye), and different CS diluents (H_2O and NaCl 0.9%). In the CS dilution in NaCl 0.9% the pH was adjusted to 5, thus the CS could interact with the HA after its addiction and with the mucin of the eye. [7,49,65] The formulations analyses consisted in the determinations of the yield, particle size, PdI and ZP. Results from the yield clearly shown that the formulations with the mass proportions of CS:HA of 1:1 and 1:2 for all HA with exception of 1000kDaltons HA did not present aggregation. The CS diluted in NaCl 0.9% presents a higher yield. The mass proportion of CS:HA 1:1 HA eye result in the best characteristics in terms of particle size, PdI and ZP (339 ± 11nm, a PdI of 0.220 ± 0.034 and a ZP of +44.5 ± 0.7mV, mean ± SD, n=3). These data are in agreement with previously described in the literature. [65]

This technique normally produces NPs with size in the range of 200-500nm, spherical shape and positive charged with a ZP of +30.0 to 57.0mV, which validates the obtained results and indicates that the formulations are stable. [39,45,59] Through the ZP results, we can also say that the NPs surface is mostly composed of CS. The positive ZP indicates that the NPs are positively charged what will promote the repulsion between them, keeping the formulation stable, and will also promote the interaction between the NPs and the mucin of the eye surface, which is negatively charged. This interaction will increase the retention time of the drug in the eye. [45,55,49] Relatively to PdI, it indicates the polydispersity of NPs size and has to be the lowest possible in order to promote the corneal uptake and stables formulations. [49]

After the optimization of the composition of NPs it was optimized the formulation process of production. For that, three types of homogenization were tested: manual, magnetic stirring and high shear homogenization. The results are present in Figure 3.1.

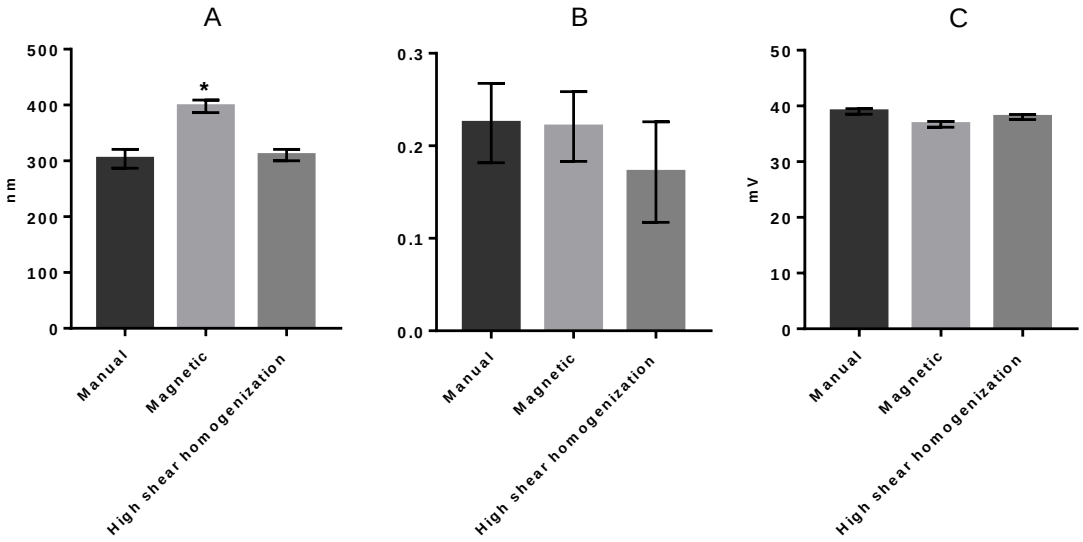

Figure 3.1: Variation of Size (A), PdI (B) and ZP (C) of NPs with CS:HA eye mass proportion of 1:1 according to different methods of homogenization (manual, magnetic stirring and high shear homogenization). There are significant differences between the size of the NPs using the different methods of homogenization *p< 0.0001 (mean ± SD, n=3).

In Figure 3.1 A, B and C it is shown that the differences between the three types of homogenization tested results in differences on the size and PdI data (Figure 3.1 A and B). In Figure 3.1 A, it is clear that the homogenization with magnetic stirring produces larger NPs when compared to the other two types of homogenization, which is highlighted by the significant changes observed. On the other hand, Figure 3.1 C shows that the magnetic stirring have lower ZP, although no significative change is observed between it and the high shear homogenization, what makes them equivalent methods. In Figure 3.1 B, no significant changes ($p>0.05$) were observed between the three methods of homogenization though the high shear homogenization show a lower value of PdI than the other methods. Analysing all the results together, the high shear homogenization presented better results for the formulation of NPs.

3.1.1. Encapsulation efficiency Evaluation

After the manufacturing process method optimized, the encapsulation of the antioxidant, crocin, and of the UV absorber, actino were evaluated. These two compounds were chosen due to their properties of ROS reduction. Since the eye is much affected by the incident of light on it [13], it is used the actino which, together with the HA, is able to absorb the UV radiation and to decrease the OS effects on the eye. [36,37] The crocin, on the other hand, is a carotenoid that is able to scavenge FRs, especially superoxide anions, reducing the ROS and consequently protecting the cell against OS. [31,32] The encapsulation efficacy is shown in Table 3.1.

Table 3.1: EE of crocin and actino and their loading for different loading amounts (mean ± SD, n=3).

	Total Concentration (µg/mL)	Encapsulation Concentration (µg/mL)	EE (%)	DL (%)
	0	**0**	**0**	**0**
Crocin	1200	**1077.1 ± 1.5**	**89.8 ± 0.1**	**0.279 ± 0.000**
	600	**449.1 ± 5.9**	**74.9 ± 1.0**	**0.112 ± 0.001**
	200	**157.5 ± 0.2**	**78.8 ± 0.2**	**0.039 ± 0.000**
	40	**9.4 ± 1.1**	**23.5 ± 2.7**	**0.002 ± 0.000**
	20	**8.9 ± 0.8**	**44.4 ± 3.8**	**0.002 ± 0.000**
	4	**3.7 ± 0.1**	**91.7 ± 2.7**	**0.001 ± 0.000**
Actino	40	**1.1 ± 3.3**	**2.6 ± 8.2**	**0.263 ± 0.820**
	20	**1.0 ± 0.7**	**4.8 ± 3.4**	**0.241 ± 0.170**
	4	**0.2 ± 1.6**	**5.6 ± 40.4**	**0.056 ± 0.404**

As it can be observed on data at Table 3.1, crocin is more efficiently encapsulated that actino, even for higher concentrations of actino the encapsulation concentration and DL do not have a significant increase. That may be explained by the interactions that the actino with the HA and the CS separately. The interaction between the actino and HA has already been studied, as referred before. [36,37] The actino and HA interaction may be affected by the bonds between HA and the CS. FTIR spectra was used to evaluate the interaction between all the components used for the CS/HA, CS/HA/crocin, CS/HA/actino and CS/HA/crocin/actino NPs (Figure 3.2). Although the actino was not efficiently encapsulated in the NP formulations, it absorbs UV radiation and it should help in the prevention of ROS formulation, studies of OS will be shown later. [36,37] The results presented in Table 3.1 show that higher the concentrations of crocin in the formulation are, higher its encapsulation concentration and consequently DL. The co-encapsulation values were not conclusive since that the crocin and actino absorb at same wavelengths (324nm and 305nm, respectively).

Before the FTIR analyses, the CS/HA/crocin, CS/HA/actino and CS/HA/crocin/actino NPs were characterized in terms of Size, PdI and ZP. The results of these tests show no significant differences between the formulations characteristics with the encapsulation of crocin and actino, agreeing with the values referred in the literature (Table 3.2). [39,45,59]

Table 3.2: Size, PdI and ZP of CS/HA, CS/HA/crocin, CS/HA/actino and CS/HA/crocin/actino NPs (mean ± SD, n=3).

	Total concentration (µg/mL)	Size (nm)	PdI	Zeta (mV)
	0	323.4 ± 9.9	0.186 ± 0.029	+37.7 ± 1.1
Crocin	**1200**	295.3 ± 1.1	0.174 ± 0.020	+38.8 ± 0.8
	600	309.2 ± 4.4	0.193 ± 0.006	+37.6 ± 0.4
	200	304.1 ± 3.1	0.196 ± 0.008	+38.9 ± 0.9
	40	296.5 ± 5.1	0.179 ± 0.020	+33.2 ± 0.9
	20	302.4 ± 5.1	0.177 ± 0.015	+35.0 ± 1.2
	4	292.4 ± 2.9	0.142 ± 0.030	+36.0 ± 2.2
Actino	**40**	316.5 ± 2.5	0.196 ± 0.009	+36.6 ± 0.5
	20	328.9 ± 4.0	0.235 ± 0.017	+36.8 ± 0.8
	4	318.6 ± 1.7	0.189 ± 0.025	+37.0 ± 0.7
	Crocin (600) + actino (40)	330.1 ± 5.5	0.232 ± 0.013	+41.0 ± 0.4

3.1.2. FTIR

For a better analysis of the interactions formed by the NP components, a FTIR analysis was made. The spectrums that resulted from this analysis are represented in Figure 3.2.

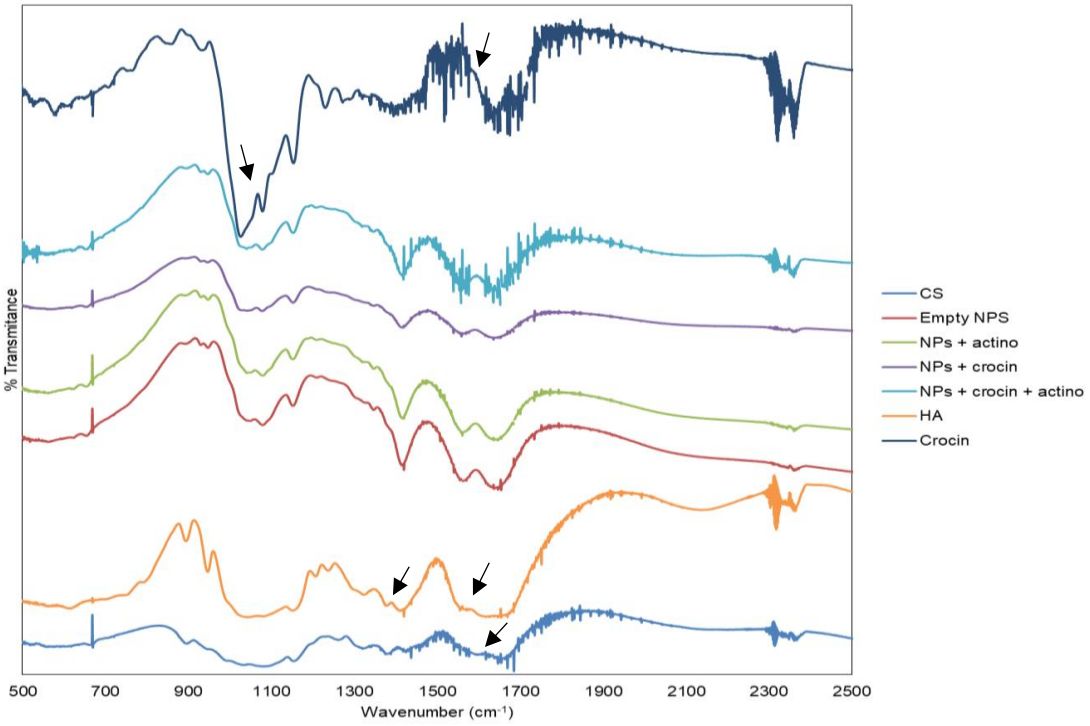

Figure 3.2: FTIR evaluation of the polymer-polymer interactions. The graphic shows the comparison between the FTIR analysis of the formulations and CS, HA eye and crocin. The black arrows represent the lengths where changes occurs.

The results obtained in Figure 3.2 demonstrate that there are some interactions between the NP components. In all the spectrums of Figure 3.2, it is possible to observe bands between 675 and 900cm^{-1} (out-of-plane bands) that are also characteristic of the aromatic substitution pattern. [66] The pure HA spectrum (orange) present a band at 1406cm^{-1} for N-H bending vibration, which is one of the characteristic bands of this compound. The bands between 1640–1690cm^{-1} present in the spectrums of pure HA and pure CS are assigned C=O stretching of amide I. This bands region is also the most characteristic of CS. [67,68] In the Figure 3.2, it is possible to identify two bands that are characteristic of the pure crocin spectrum (around 1070cm^{-1} and around 1612cm^{-1}). The band of 1070cm^{-1} is assigned to the C–O sugar groups of crocin. [69] The second band is assigned to the asymmetric and symmetric stretching peaks of carboxylic groups and slightly shifted from 1612 to 1615cm^{-1} after complexation with CS. [70] The fact that the bands referred above suffer a detour in the spectrums of the NP formulations in comparison with the spectrums of the pure compounds show that there are some kind of interaction between the NP's components (covalent and non-covalent bonds).

3.1.3. TEM

The morphology of the NPs was evaluated by TEM. It creates a high-energy electron beam, which produces an image when it is transmitted through the sample. [71] The results are shown in Figure 3.3.

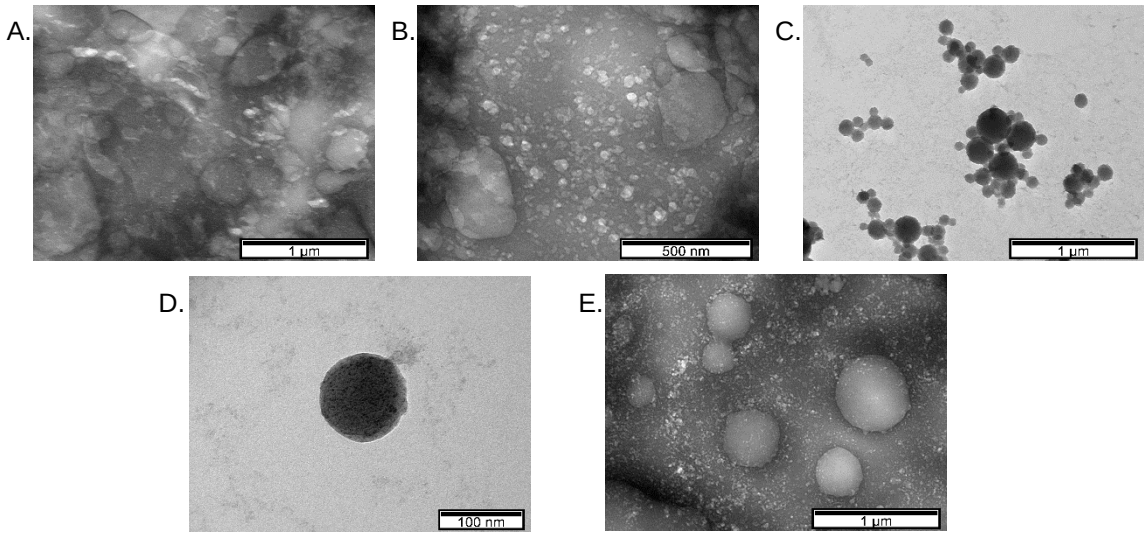

Figure 3.3: TEM evaluation of CS/HA (A), CS/HA/crocin (B), CS/HA/actino (C and D) and CS/HA/crocin/actino (E) NPs.

The Figure 3.3 A and B present NPs without a clear shape that may be due to the technique itself since the electron beam can damage the sample. However, it is possible to identify some NPs in the image (white dots). On the other hand, the Figure 3.3 C, D and E show NPs with a spherical morphology, which is in agreement with the described shape of this kind of NPs in the literature. [45] This can been better seen in image D for it has a higher amplification. The Figure 3.3 C, as well as Figure 3.3 E, also show the polydispersity of shapes that can be

obtained in one sample of NPs. TEM images seems to show that none of the compounds changes the initial obtained formulations but there were necessary more studies to conform it.

3.2. Stability Test

The stability test is essential to evaluate how much time the NP formulations will maintain their properties and will be viable to be used as a drug delivery system. Therefore, the measurement of the NPs size, PdI and ZP was made at 0, 8, 15 and 32 days after they had been formulated. The results are shown in Figure 3.4.

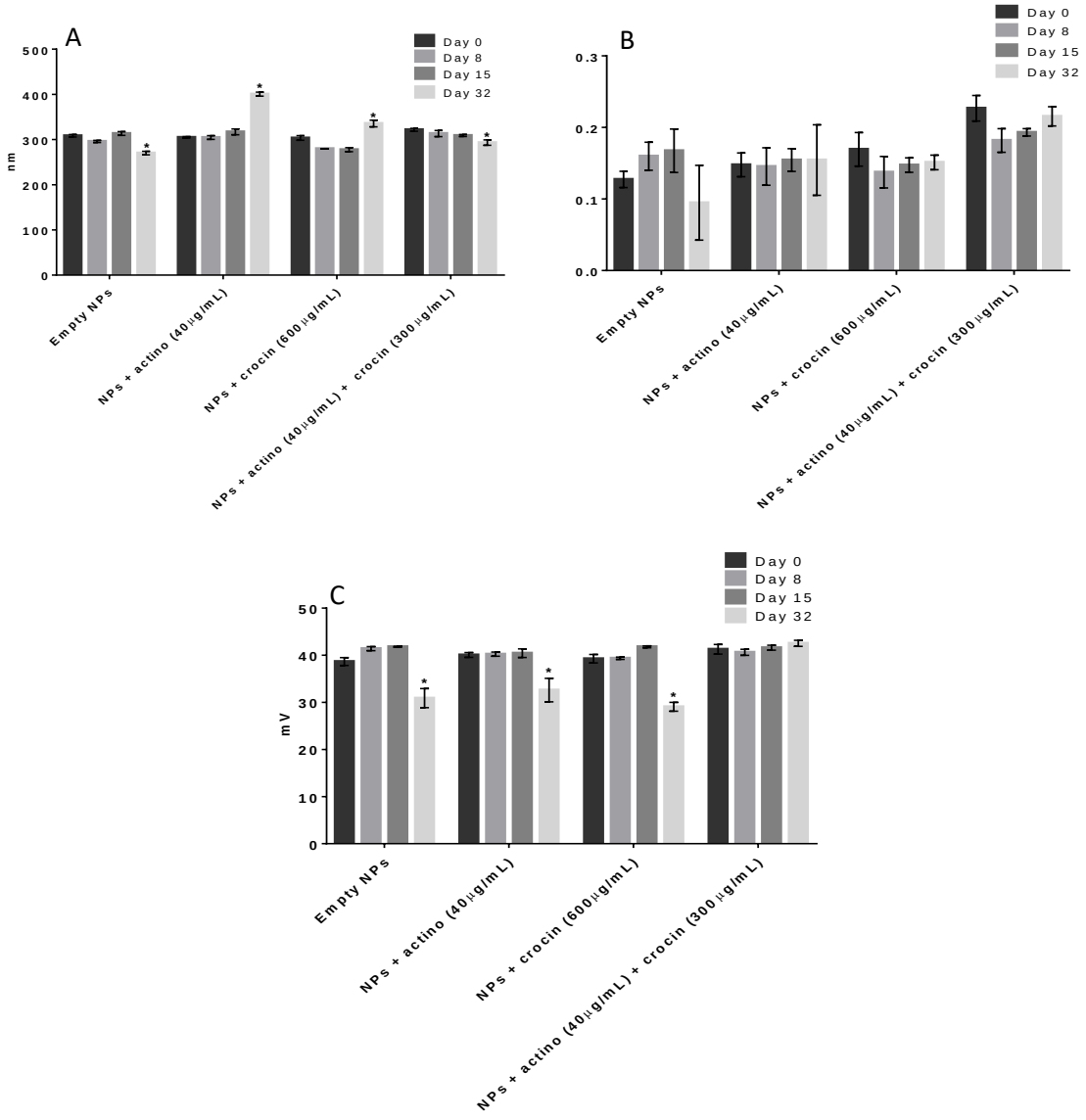

Figure 3.4: Stability results of the formulations size (A), PdI (B) and ZP (C). Data compared with time zero. There are significant differences between the size of the NPs analysed at different times *p< 0.0001, the same significant differences are observed in the ZP of the NPs (mean ± SD, n=3).

The study shows that all the NPs destabilized after 32 days of production, showing significant changes in both size and ZP values. In the Figure 3.4 A, the NPs loaded with crocin have a significant reduce of their size on days 8 and 15, which can be justified by the crocin

release of the NPs. The same happens with NPs loading with both crocin and actino, but with less level of significance. This phenomenon will be studied later in the release studies.

3.3. In vitro Assays

3.3.1. Cytotoxicity

The cytotoxicity of the formulations is another very important aspect in the development of a drug delivery system. So, as the developed formulations are for ophthalmic application, it was used the ARPE-19 cell line, a primary RPE culture, by measures its cell viability by the evaluation of the metabolic cell state and cell membrane integrity, after the formulations been applied. [58] For the membrane integrity it was used PI dye uptake and for the metabolic state it was used Alamar Blue and MTT dyes (Figure 3.5).

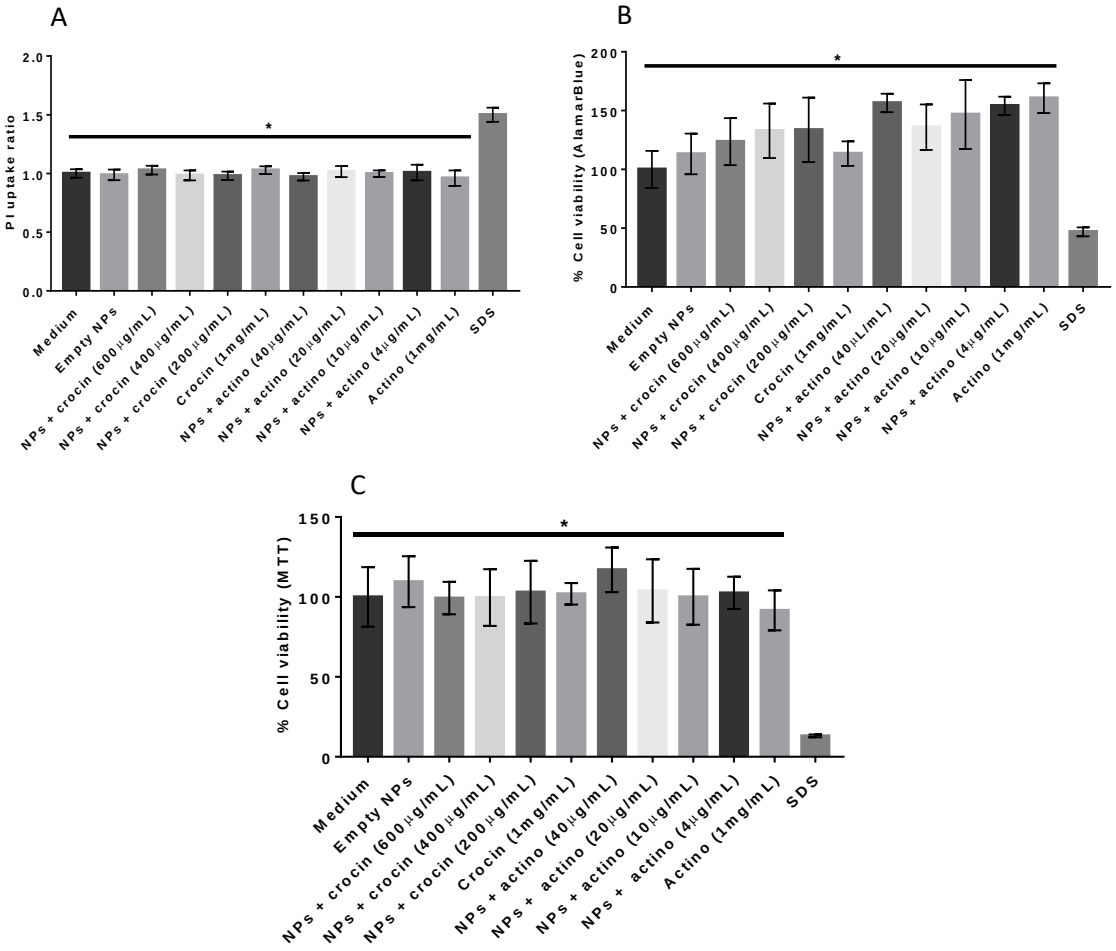

Figure 3.5: Evaluation of cytotoxicity of the NPs at different concentrations by PI uptake ratio (A) and percentage of cell viability measured by Alamar Blue (B) and MTT (C) in ARPE-19 cell line for 24h of exposition time. There are significant differences between the groups of samples tested and the positive control SDS *p< 0.0001. (mean ± SD, n=8).

The cytotoxicity studies show that there is a significant difference between the values of SDS ($p<0.0001$), positive control of cytotoxicity, and all samples tested and a no significant difference ($p>0.05$) between the values of samples groups, for the three endpoints tested, and

the culture medium. It can be concluded and in agreement with other published studies [31,37,45] that this NPs do not present cytotoxicity for the tested cell line.

3.4. *In vitro* release and permeation studies

The release and permeation studies were only performed for the NPs loaded with crocin, since the actino performs its function at surface eye. [36,37]

3.4.1. Dialyses membranes

The results of cumulative amount of crocin released through the membrane are shown in Figure 3.6.

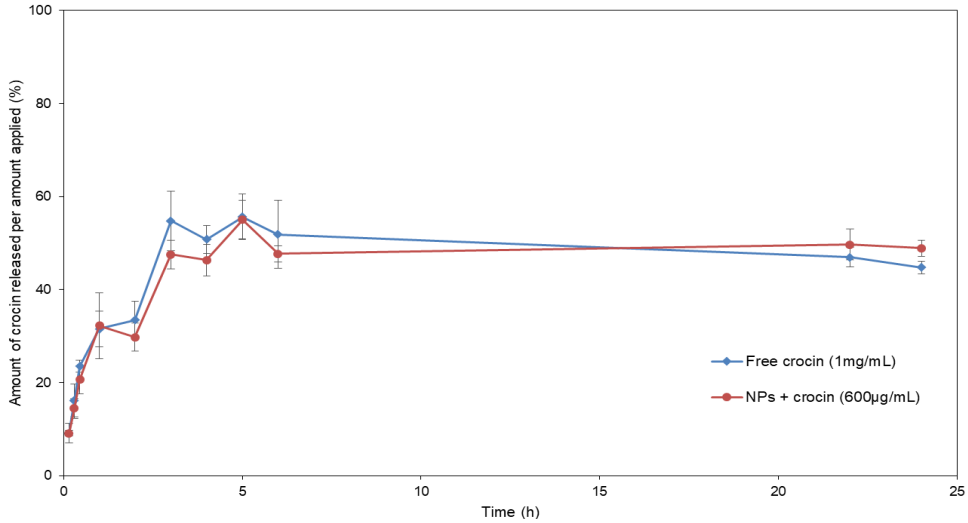

Figure 3.6: Percentage of the amount of crocin released per amount applied. NP loaded with crocin (red) and a free crocin solution (blue) in 10mM PBS pH 7.4 through a dialyses membrane at room temperature. (mean ± SD, n =3).

As it is shown in Figure 3.6, the crocin was absorbed in the dialyze membranes and never reaches 100% of release.

3.4.2. Franz Diffusion Cells

In order to evaluate the release kinetics and permeation profile, it was performed a release and permeation studies of NPs loaded with crocin in Franz diffusion cells, using cellulose membranes and scleras from pig eyes. The results are given in Figure 3.7.

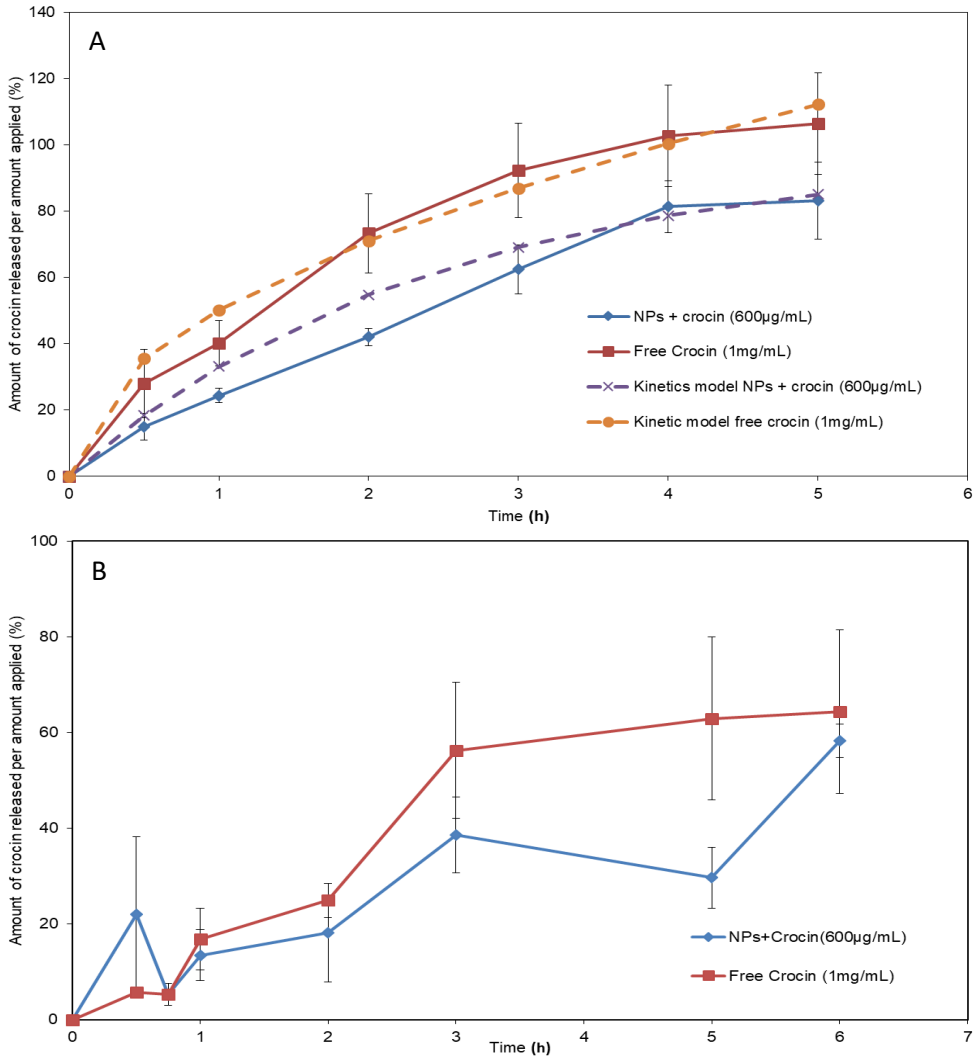

Figure 3.7: Release profiles in a cellulose membrane of NP loaded with crocin (blue), a free crocin solution (red) and the correspondent kinetic profile of release (purple and orange, respectively) in 10 mM PBS pH 7.4 through Franz Cells at 37ºC (A). Permeation profile in scleras of pig eyes (B) in 10 mM PBS pH 7.4 through Franz Cells at 37ºC. (mean ± SD, n=6)

The *in vitro* release profile of crocin revealed (Figure 3.7 A) a controlled drug release from the NPs. The use of pH 7.4 is due to the normal tear present a pH mean value of 7.4. [7]

In Figure 3.7 A and B, the incorporation of crocin in the NP formulations decreased its velocity of release and the amount of crocin released. According to Figure 3.7 B, there is a slow permeation of crocin in the initial hours, which is possibly due to its interaction with the sclera constitutes (this can be supported by the color present in the pig eye elements after the conclusion of the study).

The drug release kinetics were characterized by fitting the experimental results to different kinetic models. The best fitted model (with the highest determination coefficient, R^2, and lowest values for Akaike Information Criterion, AIC), to the releases data using cellulose membranes is the Higuchi model for the free crocin solution and the first order model for the NPs loaded with

crocin (Table 3.3). For the free crocin solution the best fitting was obtained with the Higuchi square root model ($R^2_{adjusted}$ = 0.870), with slightly lower values for the First order model (0.801) (Table 3.3). Regarding the NPs loaded with crocin, First order model exhibits the best fitting ($R^2_{adjusted}$ = 0.855) when compared to the Korsmeyer-Peppas model (0.820) with close but distinct AIC values, with the First model presenting a clear minimum (Table 3.3). In fact, the dissolution profile is suggestive of a diffusion-controlled release over time period. According to Higuchi, this behavior is due to the dispersion of crocin in a homogeneous and uniform matrix, which acts as the diffusional. [72] In addition, the first order explains the polymer dissolution at the interface with the surrounding medium, enhancing the drug mobility and diffusion. [73,74]

Table 3.3: Mathematical models and respective parameters (correlation coefficients and release constants) obtained from the fitting of the experimental data corresponding to a crocin release from CS/HA NPs.

		Free crocin	**NPs + crocin**
Zero order	R^2_{adj}	0.680	0.770
	AIC	46.907	43.275
	k0 (µg/h)	26.212	20.546
First order	R^2_{adj}	0.801	0.855
	AIC	44.277	39.479
	k1 (h^{-1})	0.743	0.407
Higuchi	R^2_{adj}	0.870	0.801
	AIC	41.941	43.081
	kH ($h^{-0.5}$)	50.203	38.853
Korsmeyer-Peppas	R^2_{adj}	0.779	0.820
	AIC	44.199	42.753
	kKP (h^n)	48.473	29.720
	N	0.576	0.731

3.5. Mucoadhesion studies

3.5.1. Ostwald viscometer

The Ostwald viscometer was used to determine the viscosity of the formulations and evaluate its mucoadhesion, through their interaction with mucin. The viscosity values obtained by this method are represented in Figure 3.8.

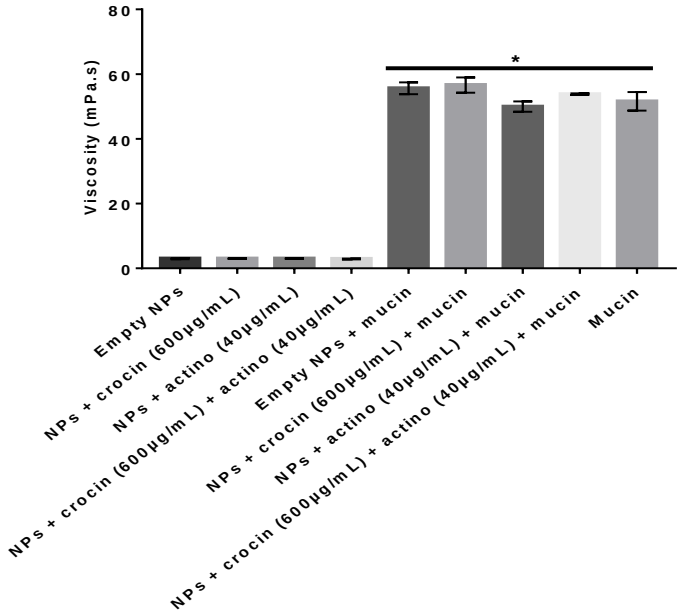

Figure 3.8: Viscosity of the formulations with and without mucin (*p< 0.0001 as compared samples with samples with mucin). (mean ± SD, n=3).

In Figure 3.8, it was possible to observe an increase of viscosity when NPs were mixed with mucin, which represent an interaction with the NPs surface. This observation supports the hypotheses that the positive charges groups of the CS, present in the NPs surface, interact with the negative charge groups of the mucin, enabling the NPs penetration into the mucin of the eye. [44,45,46,49,50] The interaction observed may result in a stronger mucoadhesivity and increases the drug retention time in the eyes, which improves the drug absorption and can reduce the frequency of administration. [45,46,47,49,50] No significative changes were observed between the samples with mucin.

3.5.2. Rotational Rheometer

Tackiness in the context of material behaviour is associated with stickiness and may result from adhesive forces between two materials in contact. It is measured at the maximum force needed to break the resultant bond. In this method, the peak normal force (N), which is a negative normal force, can be attributed to tack and the area under the force time curve (N.s) represents the adhesive strength. [75] These parameters are measured and the results of the tested formulations are represented in Table 3.4.

Table 3.4: Analyses of the mucoadhesion of the formulations with and without mucin. The mucin solution is the control of this study. (mean ± SD, n=6)

Samples	Peak normal force - Normal Force (N)	Area under force time curve (N.s)
Empty NPs	-0.132 ± 0.006	0.572 ± 0.428
NPs + crocin (600µg/mL)	-0.178 ± 0.018	0.507 ± 0.081

Samples	Peak normal force - Normal Force (N)	Area under force time curve (N.s)
NPs + actino (40µg/mL)	-0.172 ± 0.006	0.416 ± 0.100
NPs + crocin (600µg/mL) + actino (40µg/mL)	-0.178 ± 0.012	0.438 ± 0.085
Mucin	-0.166 ± 0.006	0.414 ± 0.061
Empty NPs + Mucin	-0.162 ± 0.009	0.469 ± 0.047
NPs + crocin (600µg/mL) + Mucin	-0.167 ± 0.008	0.422 ± 0.058
NPs + actino (40µg/mL) + Mucin	-0.169 ± 0.005	0.466 ± 0.069
NPs + crocin (600µg/mL) + actino (40µg/mL) + Mucin	-0.165 ± 0.003	0.479 ± 0.103

Concerning the peak normal force, the NPs + crocin (600µg/mL) + actino (40µg/mL) appears to be the tackiest of the formulations with a peak normal force of -0.178N. On the other hand, in the case of the area under the force time curve, the formulation with the more cohesive structure appears to be the Empty NPs (0.572N.s) and the mucin the less cohesive structure (0.414N.s). However, no significative changes were observed between the results for the different formulations. The results relating to mucin present peaks normal forces and areas under force time curve very similar, which could mean that the added of mucin to the formulations will make them more tackiest and cohesive. [75] These results may mean that NPs present intrinsic mucoadhesive properties conferred by the mucoadhesive polymers used in their formulation (CS and HA). [7,45,49,54]

3.5.3. Zeta Potential

Another method used for the mucoadhesion studies is the determination of ZP of the formulations with and without mucin. The results of this analysis are represented in Table 3.5.

Table 3.5: Determination of the ZP (mV) of the formulations with and without mucin. The mucin solution is the control of this study. (mean ± SD, n=3)

Samples	ZP (mV)
Empty NPs	+34.1 ± 1.9
NPs + crocin (600µg/mL)	+39.2 ± 1.3
NPs + actino (40µg/mL)	+41.4 ± 2.0
NPs + crocin (600µg/mL) + actino (40µg/mL)	+40.2 ± 1.6
Mucin	-7.0 ± 0.2
Empty NPs + Mucin	-9.7 ± 1.1
NPs + crocin (600µg/mL) + Mucin	-9.3 ± 0.3
NPs + actino (40µg/mL) + Mucin	-10.4 ± 0.6
NPs + crocin (600µg/mL) + actino (40µg/mL) + Mucin	-9.3 ± 0.4

These results show that when the NP formulations are mixed with the mucin solution there is a reduction of ZP to negative values. Although these observations, no significative

changes were obtained between the formulations without mucin, as well as, between the formulations with mucin. These results reveal that there is an interaction between the NPs and the mucin. The mucoadhesive properties of the formulations is due to an interaction between the positive charge groups of CS and negative charge groups of mucin (ionic interaction), facilitating the NPs penetration into the structure of the mucin of the eye. [44,45,46,49,50] This ionic interaction decreases the ZP value because the mucin interact with the CS in the surface of the NPs, neutralizing the positive charges.

3.6. In vitro Assays

3.6.1. Oxidative stress tests

With all the other characteristics of the drug delivery system being already studied, it is only missing the analyses of the protection that this system gives to the cells against the OS, through the reducing of ROS. In this study, the induction of ROS production in the ARPE-19 cell line was carried out by chemical induction (H_2O_2) and physical induction (UV radiation incidence). [12,13,14,15,17,18]

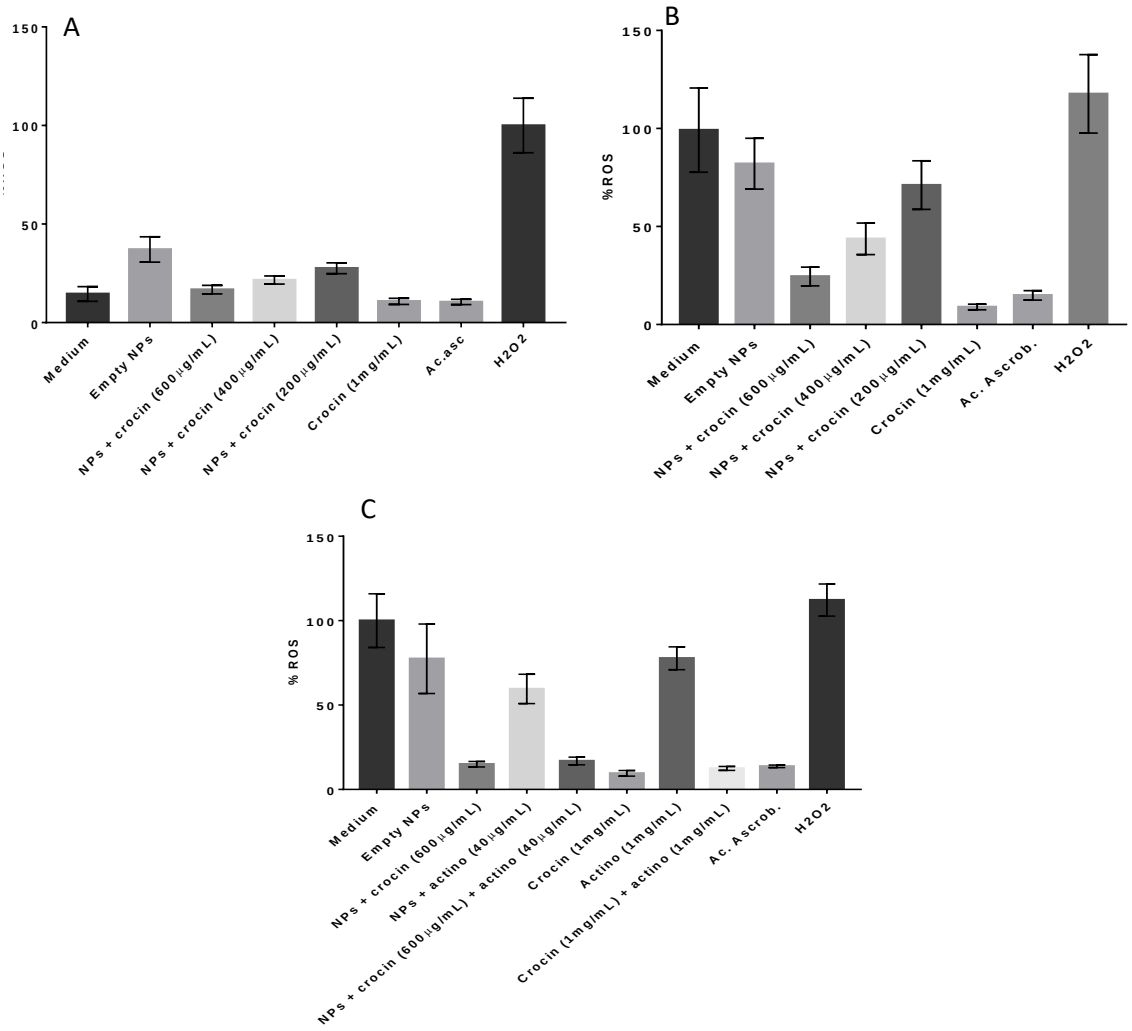

Figure 3.9: Data of the percentage of ROS in ARPE-19 cell line with and without formulations and different methods for the induction of ROS production, chemical induction (H_2O_2) and physical induction (UV radiation incidence). For the formulations loaded with crocin it was use the two methods of induction (A and B) and

for the formulations loaded with actino and with crocin and actino it was only used the physical induction (C) (mean ± SD, n=8).

The Figure 3.9 clearly shows that crocin has a powerful antioxidant activity that, when in the appropriate concentrations, presents similar values of ROS reduction as the ascorbic acid. It also shows that the crocin, being loaded in CS/HA NPs does not affect its antioxidant effect on the cells. According to results obtained in Figure 3.9, the actino revealed its protective action against UV radiation, although it is not effective for ROS reduction. The use of CS/HA NPs loaded with crocin and actino also present an activity against ROS production, which means that these formulations are suitable to prevent the OS in the cells and consequently the associated neurodegenerative diseases in the eye. [31,32,36,37,39]

3.6.2. Nanoparticles uptake

To study the interaction between the dispersion of NPs and ARPE-19 cells, it was carried out an uptake study. The CS of the NP formulations was marked with oregon green and there were used two other dyes, DAPI for the nucleus and Phalloidin-TRITC for the actin, an element of the cytoskeleton of the cells. The images resulting from the fluorescent microscopy observation are in Table 3.6.

Table 3.6: Uptake of CS/HA NPs, CS/HA NPs loaded with actino, CS/HA NPs loaded with crocin and CS/HA NPs loaded with both crocin and actino in the ARPE-19 cell line. To obtain the images three markers were used one for the nucleus (DAPI in blue), for the actin (Phalloidin-TRITC in red) and the for the NPs (CS marked with Oregon Green in green). Scale bar 20 µm.

Sample	Nuclei (DAPI)	Actin (Phalloidin-TRIC)	Particles (Oregon Green)	Combined (all channels)
Control	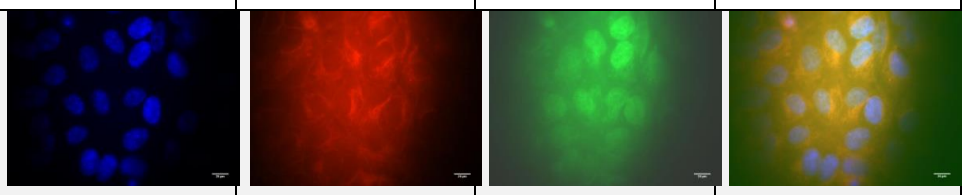			
Empty NPs	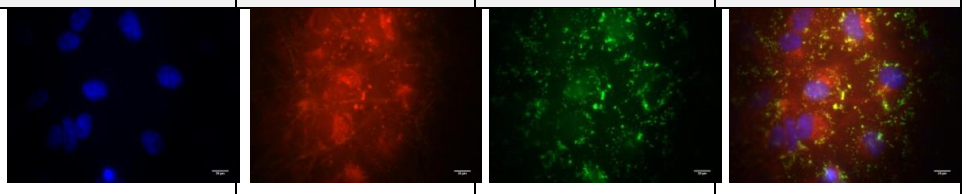			
NPs + crocin	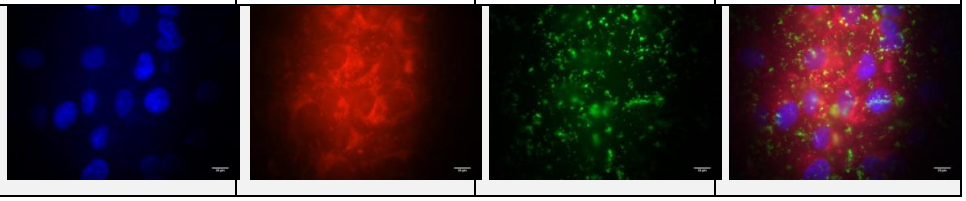			

Sample	Nuclei (DAPI)	Actin (Phalloidin-TRIC)	Particles (Oregon Green)	Combined (all channels)
NPs + actino	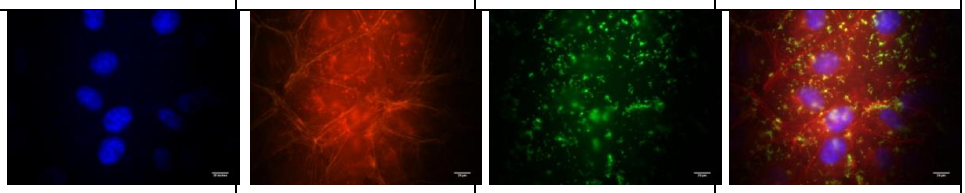			
NPs + crocin +actino	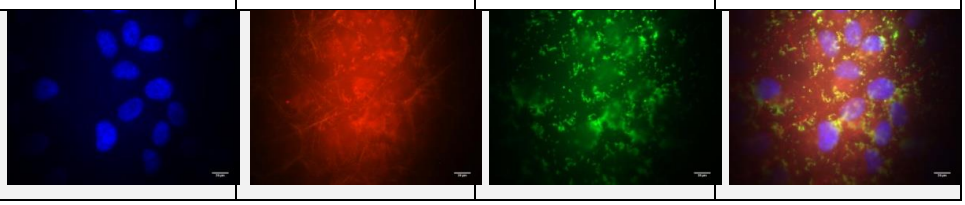			

The Table 3.6 demonstrate that there is the uptake of the NPs by the cells, with them being within the actin structure (red), and their dispersion in the cell structure (green), with tendency to get close to the cell nucleus (blue). The NPs get close to the nucleus to release the antioxidant and prevent the action of ROS, as well as, its formation.

4. Conclusions and Future Perspectives

This present study tried to develop novel NP systems with mucoadhesive properties, intended to encapsulate antioxidant molecules and, aiming to reduce the generation of OS and consequently ocular diseases. Our strategy involved the use of NPs composed by CS and HA, with known mucoadhesive properties, as a way to improve the retention time of antioxidant molecules on the surface of the eye.

The CS/HA NPs is a promising platform for antioxidants delivery in the eye by increasing its residence time and controlled drug delivery. They presented suitable mean average size (<350nm), Pdi (<0.300), surface charge (>+30mV) and also presented high EE of crocin, a powerful antioxidant, without significantly changing their properties. This drug delivery system present suitable release and mucoadhesive properties, it can reduce efficiently the ROS present in the cells and it is nontoxic to the ARPE-19 cell culture.

In the future, *in vitro* experiments would be useful to elucidate the biodistribution of drugs after ophthalmic application. Additionally, structural studies using X-ray photoelectron spectroscopy and nuclear magnetic resonance (NMR) spectroscopy techniques would complement the physicochemical characterization of the CS/HA NPs. Another objective will be the scale-up of the manufacturing processes using a Quality by Design approach, assuring the quality of the drug product and cost-effectiveness.

5. References

[1] Kim, Y., Chiang, B., Wu, X. and Prausnitz, M. (2014). Ocular delivery of macromolecules. *Journal of Controlled Release*, 190, pp.172-181.

[2] Kumar, A., Malviya, R. and Sharma, P.K. (2011). Recent Trends in Ocular Drug Delivery: A Short Review. *European Journal of Applied Sciences*, 3(3), pp. 86–92.

[3] National Eye Institute. Facts About the Cornea and Corneal Disease. Available at: https://nei.nih.gov/health/cornealdisease [Accessed 28 Jul. 2019].

[4] Health Life Media. Understanding The Eye: Anatomy. Healthlifemedia.com. Available at: http://healthlifemedia.com/healthy/understanding-the-eye-anatomy [Accessed 28 Jul. 2019].

[5] London, A., Benhar, I. and Schwartz, M. (2012). The retina as a window to the brain—from eye research to CNS disorders. *Nature Reviews Neurology*, 9(1), pp.44-53.

[6] Collins Street Optometrists. Understanding the Tear Film and Dry Eye. Available at: https://www.collinsoptometrists.com.au/dry-eye-clinic/understanding-the-tear-film-and-dry-eye/ [Accessed 28 Jul. 2019].

[7] LUDWIG, A. (2005). The use of mucoadhesive polymers in ocular drug delivery. *Advanced Drug Delivery Reviews*, 57(11), pp.1595-1639.

[8] Bron, A., Tiffany, J., Gouveia, S., Yokoi, N. and Voon, L. (2004). Functional aspects of the tear film lipid layer. *Experimental Eye Research*, 78(3), pp.347-360.

[9] Foulks, G. (2007). The Correlation Between the Tear Film Lipid Layer and Dry Eye Disease. *Survey of Ophthalmology*, 52(4), pp.369-374.

[10] Cwiklik, L. (2016). Tear film lipid layer: A molecular level view. *Biochimica et Biophysica Acta (BBA) - Biomembranes*, 1858(10), pp.2421-2430.

[11] Dartt, D. and Willcox, M. (2013). Complexity of the tear film: Importance in homeostasis and dysfunction during disease. *Experimental Eye Research*, 117, pp.1-3.

[12] Umapathy, A., Donaldson, P. and Lim, J. (2013). Antioxidant Delivery Pathways in the Anterior Eye. *BioMed Research International*, 2013, pp.1-10.

[13] Saccà, S., Roszkowska, A. and Izzotti, A. (2013). Environmental light and endogenous antioxidants as the main determinants of non-cancer ocular diseases. *Mutation Research/Reviews in Mutation Research*, 752(2), pp.153-171.

[14] Tezel, G. (2009). The Role of Glia, Mitochondria, and the Immune System in Glaucoma. *Investigative Opthalmology & Visual Science*, 50(3), p.1001.

[15] Uttara, B., Singh, A., Zamboni, P. and Mahajan, R. (2009). Oxidative Stress and Neurodegenerative Diseases: A Review of Upstream and Downstream Antioxidant Therapeutic Options. *Current Neuropharmacology*, 7(1), pp.65-74.

[16] Bull, N. and Martin, K. (2011). Concise Review: Toward Stem Cell-Based Therapies for Retinal Neurodegenerative Diseases. *STEM CELLS*, 29(8), pp.1170-1175.

[17] Cabrera, M. and Chihuailaf, R. (2011). Antioxidants and the Integrity of Ocular Tissues. *Veterinary Medicine International*, 2011, pp.1-8.

[18] Simonian, N. and Coyle, J. (1996). Oxidative Stress in Neurodegenerative Diseases. *Annual Review of Pharmacology and Toxicology*, 36(1), pp.83-106.

[19] Delcourt, C., Cristol, J. P., L´eger, C. L., Descomps, B., and Papoz, L. (1999). Associations of antioxidant enzymes with cataract and age-related macular degeneration: the POLA study. *Ophthalmology*, 106(2), p.215–222.

[20] Lyle, B. J., Mares-Perlman, J. A., Klein, B. E. K. et al. (1999). Serum carotenoids and tocopherols and incidence of age-related nuclear cataract. *American Journal of Clinical Nutrition*, 69(2), p.272–277.

[21] Gale, C. R., Hall, N. F., Phillips, D. I. W., and Martyn, C. N. (2001). Plasma antioxidant vitamins and carotenoids and age-related cataract. *Ophthalmology*, 108(11), p.1992–1998.

[22] Jacques, P. F., Chylack Jr., L. T., Hankinson, S. E. et al. (2001). Long-term nutrient intake and early age-related nuclear lens opacities. *Ophthalmology*, 119(7), p.1009–1019.

[23] Berendschot, T. T. J. M., Broekmans, W. M. R., Kl¨opping-Ketelaars, I. A. A., Kardinaal, A. F. M., Poppel, G., and Norren, D. (2002). Lens aging in relation to nutritional determinants and possible risk factors for age-related cataract. *Archives of Ophthalmology*, 120(12), p.1732–1737.

[24] Delcourt, C., Carri`ere, I., Delage, M., Descomps, B., Cristol, J. P., and Papoz, L. (2003). Associations of cataract with antioxidant enzymes and other risk factors: the French age-related eye diseases (POLA) prospective study. *Ophthalmology*, 110(12), p.2318–2326.

[25] Akuffo, K., Beatty, S., Peto, T., Stack, J., Stringham, J., Kelly, D., Leung, I., Corcoran, L. and Nolan, J. (2017). The Impact of Supplemental Antioxidants on Visual Function in Nonadvanced Age-Related Macular Degeneration: A Head-to-Head Randomized Clinical Trial. *Investigative Opthalmology & Visual Science*, 58(12), p.5347.

[26] Stringham, N., Holmes, P. and Stringham, J. (2017). Supplementation with macular carotenoids reduces psychological stress, serum cortisol, and sub-optimal symptoms of physical and emotional health in young adults. *Nutritional Neuroscience*, 21(4), pp.286-296.

[27] Stringham, J., O'Brien, K. and Stringham, N. (2017). Contrast Sensitivity and Lateral Inhibition Are Enhanced With Macular Carotenoid Supplementation. *Investigative Opthalmology & Visual Science*, 58(4), p.2291.

[28] Choi, R., Gorusupudi, A., Wegner, K., Sharifzadeh, M., Gellermann, W. and Bernstein, P. (2017). Macular Pigment Distribution Resposes to High-Dose Zeaxanthin Supplementation in Patients with Macular Telangiectasia Type 2. *Retina*, 37(12), pp.2238-2247.

[29] Suzuki, K. (2009). Anti-oxidants for therapeutic use: Why are only a few drugs in clinical use?. *Advanced Drug Delivery Reviews*, 61(4), pp.287-289.

[30] Natesan, S., Pandian, S., Ponnusamy, C., Palanichamy, R., Muthusamy, S. and Kandasamy, R. (2017). Co-encapsulated resveratrol and quercetin in chitosan and peg modified chitosan nanoparticles: For efficient intra ocular pressure reduction. *International Journal of Biological Macromolecules*, 104, pp.1837-1845.

[31] Abe, K. and Saito, H. (2000). Effects of saffron extract and its constituent crocin on learning behaviour and long-term potentiation. *Phytotherapy Research*, 14(3), pp.149-152.

[32] Amin, A., A. Hamza, A., Daoud, S., Khazanehdari, K., Al Hrout, A., Baig, B., Chaiboonchoe, A., E. Adrian, T., Zaki, N. and Salehi-Ashtiani, K. (2016). Saffron-Based Crocin Prevents Early Lesions of Liver Cancer: *In vivo*, *in vitro* and Network Analyses. *Recent Patents on Anti-Cancer Drug Discovery*, 11(1), pp.121-133.

[33] Ochiai, T., Shimeno, H., Mishima, K., Iwasaki, K., Fujiwara, M., Tanaka, H., Shoyama, Y., Toda, A., Eyanagi, R. and Soeda, S. (2007). Protective effects of carotenoids from saffron on neuronal injury in vitro and in vivo. *Biochimica et Biophysica Acta (BBA) - General Subjects*, 1770(4), pp.578-584.

[34] Moghaddasi, M. (2010). Saffron chemicals and medicine usage. *Journal of Medicinal Plants Research*, 4(6), pp.427-430.

[35] Laabich, A., Vissvesvaran, G., Lieu, K., Murata, K., McGinn, T., Manmoto, C., Sinclair, J., Karliga, I., Leung, D., Fawzi, A. and Kubota, R. (2006). Protective Effect of Crocin against Blue Light– and White Light–Mediated Photoreceptor Cell Death in Bovine and Primate Retinal Primary Cell Culture. *Investigative Ophthalmology & Visual Science*, 47(7), pp.3156.

[36] Čejke, Č., Luyckx, J. and Čejkova, J. (2012). Central Corneal Thickness Considered an Index of Corneal Hydration of the UVB Irradiated Rabbit Cornea as Influenced by UVB Absorber. *Physiological Research*, 61, pp. 299-306.

[37] Čejka, Č., Luyckx, J., Ardan, T., Pláteník, J., Širc, J., Michálek, J. and Čejková, J. (2010). The Effect of Actinoquinol with Hyaluronic Acid in Eye Drops on the Optical Properties and Oxidative Damage of the Rabbit Cornea Irradiated with UVB Rays. *Photochemistry and Photobiology*, 86(6), pp.1294-1306.

[38] DELAMO, E. and URTTI, A. (2008). Current and future ophthalmic drug delivery systems A shift to the posterior segment. *Drug Discovery Today*, 13(3-4), pp.135-143.

[39] Tsai, C., Wang, P., Lin, I., Huang, H., Liu, G. and Tseng, C. (2018). Ocular Drug Delivery: Role of Degradable Polymeric Nanocarriers for Ophthalmic Application. *International Journal of Molecular Sciences*, 19(9), p.2830.

[40] Liu, S., Jones, L. and Gu, F. (2012). Nanomaterials for Ocular Drug Delivery. *Macromolecular Bioscience*, 12(5), pp.608-620.

[41] Mohanraj, V. and Chen, Y. (2006). Nanoparticles - A review. *Tropical Journal of Pharmaceutical Research*, 5(1), pp.561-573.

[42] Sahoo, S., Dilnawaz, F. and Krishnakumar, S. (2008). Nanotechnology in ocular drug delivery. *Drug Discovery Today*, 13(3-4), pp.144-151.

[43] Giuliano, E., Paolino, D., Fresta, M. and Cosco, D. (2018). Mucosal Applications of Poloxamer 407-Based Hydrogels: An Overview. *Pharmaceutics*, 10(3), p.159.

[44] Donnelly, R., Shaikh, R., Raj Singh, T., Garland, M. and Woolfson, A. (2011). Mucoadhesive drug delivery systems. *Journal of Pharmacy and Bioallied Sciences*, 3(1), p.89.

[45] Silva, M., Calado, R., Marto, J., Bettencourt, A., Almeida, A. and Gonçalves, L. (2017). Chitosan Nanoparticles as a Mucoadhesive Drug Delivery System for Ocular Administration. *Marine Drugs*, 15(12), p.370.

[46] Kashikar, V.S. (2011). Ophthalmic Mucoadhesive Polymers - A Literature Review. *International Journal of Pharmaceutical Sciences Review and Research*, 7, 68–73.

[47] SaraswathiI, B., Balaji, A. and Umashankar, M. (2013). Polymers in Mucoadhesive Drug Delivery System-Latest Updates. *International Journal of Pharmacy and Pharmaceutical Sciences*, 5(3), pp.423-430.

[48] Bonacucina, G., Martelli, S. and Palmieri, G. (2004). Rheological, mucoadhesive and release properties of Carbopol gels in hydrophilic cosolvents. *International Journal of Pharmaceutics*, 282(1-2), pp.115-130.

[49] Almeida, H., Amaral, M., Lobão, P., Silva, A. and Loboa, J. (2014). Applications of Polymeric and Lipid Nanoparticles in Ophthalmic Pharmaceutical Formulations: Present and Future Considerations. *Journal of Pharmacy & Pharmaceutical Sciences*, 17(3), p.278.

[50] Menchicchi, B., Fuenzalida, J., Hensel, A., Swamy, M., David, L., Rochas, C. and Goycoolea, F. (2015). Biophysical Analysis of the Molecular Interactions between Polysaccharides and Mucin. *Biomacromolecules*, 16(3), pp.924-935.

[51] Choi, J., Kim, J., Li, Z., Oh, H., Ahn, K. and Yoon, K. (2015). Efficacy of the Mineral Oil and Hyaluronic Acid Mixture Eye Drops in Murine Dry Eye. *Korean Journal of Ophthalmology*, 29(2), p.131.

[52] Apaolaza, P., Delgado, D., Pozo-Rodríguez, A., Gascón, A. and Solinís, M. (2014). A novel gene therapy vector based on hyaluronic acid and solid lipid nanoparticles for ocular diseases. *International Journal of Pharmaceutics*, 465(1-2), pp.413-426.

[53] Kogan, G., Šoltés, L., Stern, R. and Gemeiner, P. (2006). Hyaluronic acid: a natural biopolymer with a broad range of biomedical and industrial applications. *Biotechnology Letters*, 29(1), pp.17-25.

[54] Salzillo, R., Schiraldi, C., Corsuto, L., D'Agostino, A., Filosa, R., De Rosa, M. and La Gatta, A. (2016). Optimization of hyaluronan-based eye drop formulations. *Carbohydrate Polymers*, 153, pp.275-283.

[55] Yu, T., Andrews, G. and Jones, D. (2014). Mucoadhesion and Characterization of Mucoadhesive Properties. *Mucosal Delivery of Biopharmaceuticals*, pp.35-58.

[56] Kapałczyńska, M., Kolenda, T., Przybyła, W., Zajączkowska, M., Teresiak, A., Filas, V., Ibbs, M., Bliźniak, R., Łuczewski, Ł. and Lamperska, K. (2016). 2D and 3D cell cultures – a comparison of different types of cancer cell cultures. *Archives of Medical Science*, 14(4), pp.910–919.

[57] Edmondson, R., Broglie, J., Adcock, A. and Yang, L. (2014). Three-Dimensional Cell Culture Systems and Their Applications in Drug Discovery and Cell-Based Biosensors. *ASSAY and Drug Development Technologies*, 12(4), pp.207-218.

[58] Dunn, K., Aotaki-Keen, A., Putkey, F. and Hjelmeland, L. (1995). ARPE-19, A Human Retinal Pigment Epithelial Cell Line with Differentiated Properties. *Experimental Eye Research*, 62(2), pp.155-170.

[59] Cadete, A., Figueiredo, L., Lopes, R., Calado, C., Almeida, A. and Gonçalves, L. (2012). Development and characterization of a new plasmid delivery system based on chitosan–sodium deoxycholate nanoparticles. *European Journal of Pharmaceutical Sciences*, 45(4), pp.451-458.

[60] Ferreira, I.S., Bettencourt, A.F., Gonçalves, L.M., Kasper, S., Betrisey, B., Kikhney, J., Moter, A., Trampuz, A., Almeida, A.J. (2015). Activity of daptomycin- and vancomycin-loaded poly-epsilon-caprolactone microparticles against mature staphylococcal biofilms. *Internation Journal of Nanomedicine*, 10, pp.4351-4366.

[61] Gaspar, D., Faria, V., Gonçalves, L., Taboada, P., Remuñán-López, C. and Almeida, A. (2016). Rifabutin-loaded solid lipid nanoparticles for inhaled antitubercular therapy: Physicochemical and in vitro studies. *International Journal of Pharmaceutics*, 497(1-2), pp.199-209.

[62] Graça, D., Louro, H., Santos, J., Dias, K., Almeida, A., Gonçalves, L., Silva, M. and Bettencourt, A. (2017). Toxicity screening of a novel poly(methylmethacrylate)-Eudragit nanocarrier on L929 fibroblasts. *Toxicology Letters*, 276, pp.129-137.

[63] Zhang, Y., Huo, M., Zhou, J., Zou, A., Li, W., Yao, C. and Xie, S. (2010) DDSolver: an add-in program for modeling and comparison of drug dissolution profiles. *American Association of Pharmaceutical Scientist*, 12(3):263-271.

[64] Mahmoud, A., El-Feky, G., Kamel, R. and Awad, G. (2011). Chitosan/sulfobutylether-β-cyclodextrin nanoparticles as a potential approach for ocular drug delivery. *International Journal of Pharmaceutics*, 413(1-2), pp.229-236.

[65] Yang, L., Gao, S., Asghar, S., Liu, G., Song, J., Wang, X., Ping, Q., Zhang, C. and Xiao, Y. (2015). Hyaluronic acid/chitosan nanoparticles for delivery of curcuminoid and its in vitro evaluation in glioma cells. *International Journal of Biological Macromolecules*, 72, pp.1391-1401.

[66] Organic Chemistry. IR Spectroscopy Tutorial: aromatics. Available at: https://orgchemboulder.com/Spectroscopy/irtutor/aromaticsir.shtml [Accessed 14 Sep. 2019].

[67] Anisha, B., Biswas, R., Chennazhi, K. and Jayakumar, R. (2013). Chitosan–hyaluronic acid/nano silver composite sponges for drug resistant bacteria infected diabetic wounds. *International Journal of Biological Macromolecules*, 62, pp.310-320.

[68] Correia, C., Moreira-Teixeira, L., Moroni, L., Reis, R., van Blitterswijk, C., Karperien, M. and Mano, J. (2011). Chitosan Scaffolds Containing Hyaluronic Acid for Cartilage Tissue Engineering. *Tissue Engineering Part C: Methods*, 17(7), pp.717-730.

[69] Tarantilis, P., Beljebbar, A., Manfait, M. and Polissiou, M. (1998). FT-IR, FT-Raman spectroscopic study of carotenoids from saffron (Crocus sativus L.) and some derivatives. *Spectrochimica Acta Part A: Molecular and Biomolecular Spectroscopy*, 54(4), pp.651-657.

[70] Rahaiee, S., Shojaosadati, S., Hashemi, M., Moini, S. and Razavi, S. (2015). Improvement of crocin stability by biodegradeble nanoparticles of chitosan-alginate. *International Journal of Biological Macromolecules*, 79, pp.423-432.

[71] Science Direct. Transmission Electron Microscopy - an overview. Available at: https://www.sciencedirect.com/topics/food-science/transmission-electron-microscopy [Accessed 31 Jul. 2019].

[72] Paul, D. (2011). Elaborations on the Higuchi model for drug delivery. *International Journal of Pharmaceutics*, 418(1), pp.13-17.

[73] Dash, S., Murthy, P., Nath, L. and Chowdhury, P. (2010). Kinetic Modeling on Drug Release from Controlled Drug Delivery Systems. *Acta Poloniae Pharmaceutica ñ Drug Research*, 67(3), pp.217-223.

[74] Mulye, N. and Turco, S. (1995). A Simple Model Based on First Order Kinetics to Explain Release of Highly Water Soluble Drugs from Porous Dicalcium Phosphate Dihydrate Matrices. *Drug Development and Industrial Pharmacy*, 21(8), pp.943-953.

[75] Malvern Panalytical. (2015). Using a Rotational Rheometer to Assess Adhesion and Tackiness. Available at: https://www.azom.com/article.aspx?ArticleID=12166 [Accessed 30 Jul. 2019].

6. Appendices

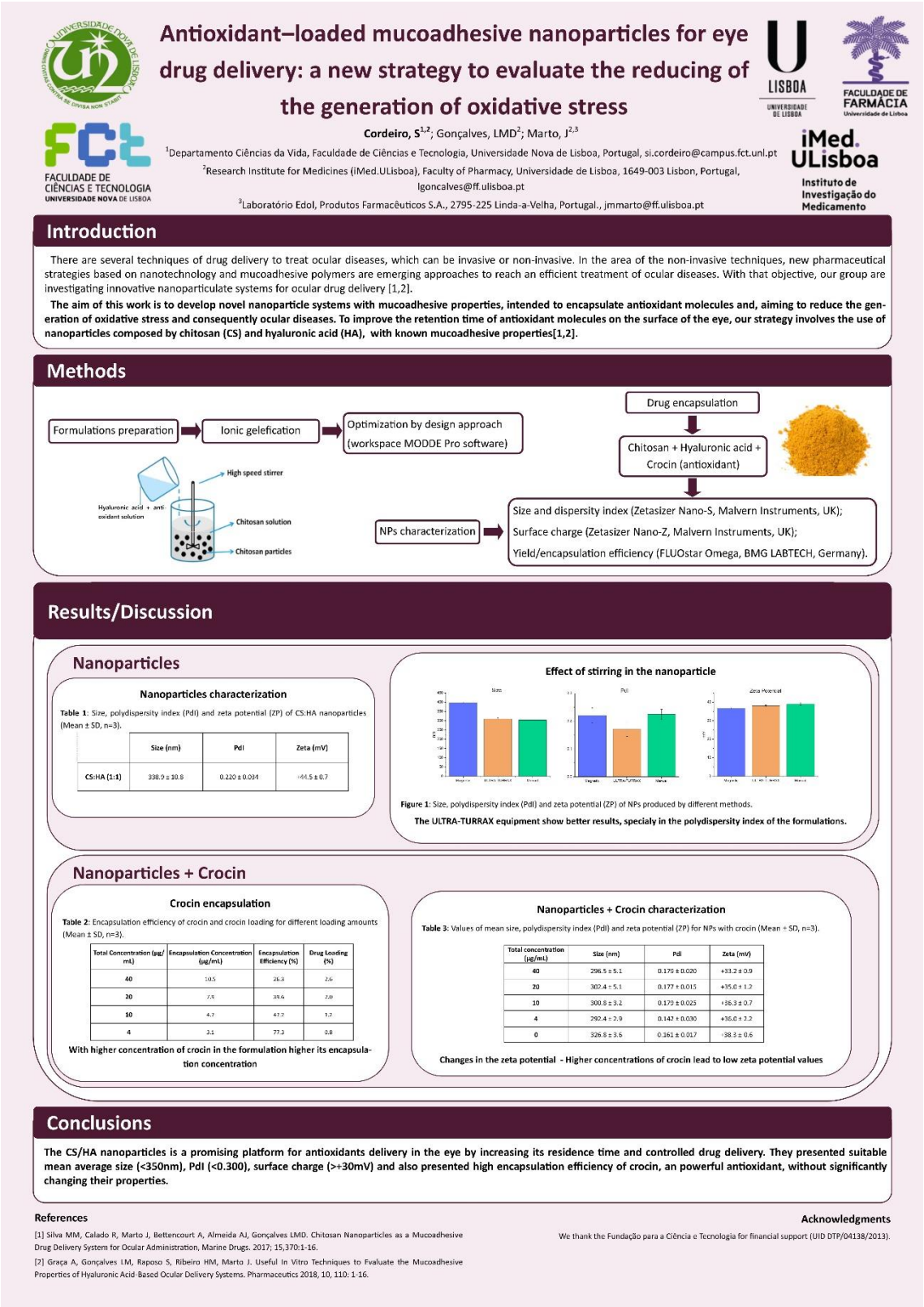

Figure 6.1: Poster presented in the scientific conference 6th IEEE Portuguese Meeting in Bioengineering (2019).

Antioxidant-loaded mucoadhesive nanoparticles for eye drug delivery: evaluating the reducing of generation of oxidative stress

Cordeiro S.[1,2], Silva B.[2,3], Gonçalves L.M.D.[2], Marto J.[2,4]

[1]Departamento Ciências da Vida, Faculdade de Ciências e Tecnologia, Universidade Nova de Lisboa, Portugal
[2]Research Institute for Medicines (iMed.ULisboa), Faculty of Pharmacy, Universidade de Lisboa, Lisbon, Portugal
[3]CIISA - Centro de Investigação Interdisciplinar em Saúde Animal, Faculty of Veterinary Medicine, Universidade de Lisboa;
[4]Laboratório Edol, Produtos Farmacêuticos S.A., 2795-225 Linda-a-Velha, Portugal

si.cordeiro@campus.fct.unl.pt

Introduction

There are several techniques of drug delivery to treat ocular diseases, which can be invasive or non-invasive. In the area of the non-invasive techniques, new pharmaceutical strategies based on nanotechnology and mucoadhesive polymers are emerging approaches to reach an efficient treatment of ocular diseases. With that objective, our group are investigating innovative nanoparticulate systems for ocular drug delivery[1,2].

The aim of this work is to develop novel nanoparticle systems with mucoadhesive properties, intended to encapsulate antioxidant molecules and, aiming to reduce the generation of oxidative stress and consequently ocular diseases. To improve the retention time of antioxidant molecules on the surface of the eye, our strategy involves the use of nanoparticles composed by chitosan (CS) and hyaluronic acid (HA), with known mucoadhesive properties.

Methods

Ionic gelefication

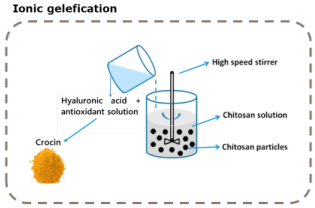

Formulations characterization

- **Size and dispersity index**
  Zetasizer Nano-S, Malvern Instruments
- **Surface charge**
  Zetasizer Nano-Z, Malvern Instruments
- **Yield/encapsulation efficiency**
  FLUOstar Omega, BMG LABTECH

Mucoadhesivity and in vitro Drug Release

- **Mucoadhesivity assays**
  Ostwald Viscometer;
  Rotational Rheometer: Kinexus Rheometer (Malvern) and a plate-plate geometry
- **Drug Release**
  Vertical Franz-type diffusion cells with artificial membranes and excised pig eye

***In vitro* studies**

- **Oxidarive stress**
  H2O2 and UV induction in ARPE-19 cell line
- **Cytotoxicity studies**
  Membrane integrity (Propidium iodide (PI) uptake) in ARPE-19 cell line
  Metabolic activity (MTT assay) in ARPE-19 cell line

Results and Discussion

Nanoparticles

Nanoparticles characterization

The proportion of CS:HA used in the formulations was 1:1 and they present a size of 338.9±10.8nm, a polydispersity index (PdI) of 0.220±0.034 and a zeta potential of +44.5±0.7mV.

Effect of stirring in the nanoparticle

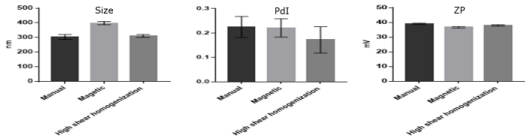

Figure 1: Size, polydispersity index (PdI) and zeta potential (ZP) of NPs produced by different methods (Mean ± SD, n=3).

The High shear homogeization show better results, specialy in the polydispersity index of the formulations

Nanoparticles + Crocin

Crocin encapsulation and Nanoparticles + Crocin Characterization

Table 1: Encapsulation efficiency of crocin and crocin loading for different loading amounts and values of mean size, polydispersity index (PdI) and zeta potential (ZP) for NPs with crocin (Mean ± SD, n=3).

Total Concentration (µg/mL)	Encapsulation Concentration (µg/mL)	Encapsulation Efficiency (%)	Drug Loading (%)	Size (nm)	PdI	Zeta (mV)
1200	1077.1 ± 1.5	89.8 ± 0.1	0.269 ± 0.0004	295.3 ± 1.1	0.174 ± 0.020	+38.8 ± 0.8
600	449.1 ± 5.9	74.9 ± 1.0	0.112 ± 0.0015	309.2 ± 4.4	0.193 ± 0.006	+37.6 ± 0.4
200	157.5 ± 0.2	78.8 ± 0.2	0.039 ± 0.00004	304.1 ± 3.1	0.196 ± 0.008	+38.9 ± 0.9
40	9.4 ± 1.1	23.5 ± 2.7	0.0023 ± 0.0003	296.5 ± 5.1	0.179 ± 0.020	+33.2 ± 0.9
4	3.7 ± 0.1	91.7 ± 2.7	0.0009 ± 0.00003	292.4 ± 2.9	0.142 ± 0.030	+36.0 ± 2.2
0	0	0	0	326.8 ± 3.6	0.161 ± 0.017	+38.3 ± 0.6

With higher concentration of crocin in the formulation higher its encapsulation concentration

Drug Release

Franz Cells

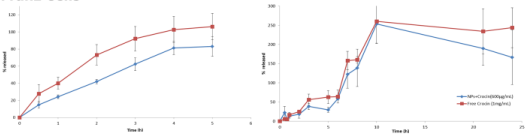

Figure 2: Release of Crocin in NPs and free form through synthetic membranes and scleras of pig eyes using Franz Cells (Mean ± SD, n=6).

Mucoadhesivity

Ostwald Viscometer

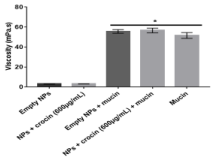

Figure 3: Viscosity of NPs in absence and presence of Mucin using the Ostwald Viscometer (Mean ± SD, n=3).

Rotational Rheometer

	Peak normal force - Normal Force (N)	Area under force time curve (N.s)
Empty NPs	-0.132 ± 0.006	0.572 ± 0.428
NPs + Crocin (600µg/mL)	-0.178 ± 0.018	0.507 ± 0.081
Mucin	-0.166 ± 0.006	0.414 ± 0.061
Empty NPs + Mucin	-0.162 ± 0.009	0.469 ± 0.047
NPs + Crocin (600µg/mL) + Mucin	-0.167 ± 0.008	0.422 ± 0.058

Table 2: Normal force and area under force time curve results for NPs and their interactions with mucin (Mean ± SD, n=6).

The results highlighted the mucoadhesivity of the formulations

In vitro studies

Oxidative stress

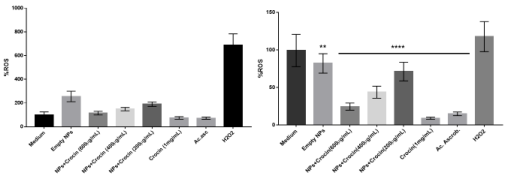

Figure 4: Percentage of ROS produced by H2O2 and UV induction in ARPE-19 cell line.

Crocin helps reducing the ROS formation

Citotoxicity

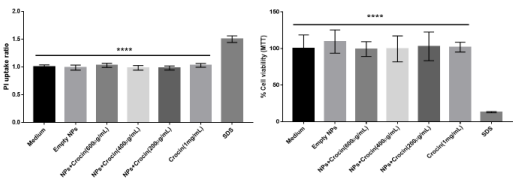

Figure 5: PI uptake and percentage of cell viability (MTT), respectively, in ARPE-19 cell line.

None of the components of the formulations is cytotoxic

Conclusions

The CS/HA nanoparticles is a promising platform for antioxidants delivery in the eye by increasing its residence time and controlled drug delivery. They presented suitable mean average size (<350nm), Pdi (<0.300), surface charge (>+30mV) and also presented high encapsulation efficiency of crocin, an powerful antioxidant, without significantly changing their properties.

References

[1] Silva MM, Calado R, Marto J, Bettencourt A, Almeida AJ, Gonçalves LMD. Chitosan Nanoparticles as a Mucoadhesive Drug Delivery System for Ocular Administration, Marine Drugs. 2017; 15,370:1-16.
[2] Graça A, Gonçalves LM, Raposo S, Ribeiro HM, Marto J. Useful In Vitro Techniques to Evaluate the Mucoadhesive Properties of Hyaluronic Acid-Based Ocular Delivery Systems. Pharmaceutics 2018, 10, 110: 1-16.

Acknowledgments

We thank the Fundação para a Ciência e Tecnologia for financial support (UID/DTP/04138/2019).

Figure 6.2: Poster presented in the scientific conferences 4rd meeting of Colégio de Química da Universidade de Lisboa, Chemistry: Shaping the Future and 11th iMed.ULisboa Postgraduate & 4th i3DU Students Meeting (2019).